System Identification of Vibrational System using GMR Sensor

Author

Danial Iltaf

Reg. # 317724

Supervisor

Dr. Mian Ashfaq Ali

DEPARTMENT OF MECHANICAL ENGINEERING

SCHOOL OF MECHANICAL & MANUFACTURING ENGINEERING

NATIONAL UNIVERSITY OF SCIENCES AND TECHNOLOGY,

ISLAMABAD

MAY 2023

System Identification of Vibrational System using GMR Sensor

Author

Danial Iltaf

Reg. # 317724

A thesis submitted in partial fulfillment of the requirements for the degree of

MS Mechanical Engineering

Thesis Supervisor:

Dr. Mian Ashfaq Ali

Thesis Supervisor’s Signature: ____________________________

DEPARTMENT OF MECHANICAL ENGINEERNG

SCHOOL OF MECHANICAL & MANUFACTURING ENGINEERING

NATIONAL UNIVERSITY OF SCIENCES AND TECHNOLOGY,

ISLAMABAD

MAY 2023

THESIS ACCEPTANCE CERTIFICATE

Certified that final copy of MS thesis written by Mr. Muhammad Umais Qamar, Registration No.31 of SMME has been vetted by undersigned, found complete in all aspects as per NUST Statutes/Regulations, is free of plagiarism, errors, and mistakes and is accepted as partial fulfillment for award of MS/MPhil degree. It is further certified that necessary amendments as pointed out by GEC members of the scholar have also been incorporated in the said thesis.

Signature with stamp: ____________________________

Name of Supervisor: Dr. Mian Ashfaq Ali

Date: 08-08-2023

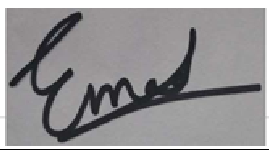

Signature of HoD with stamp: ______________________

Date: 08-08-2023

Countersign by

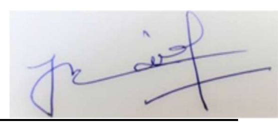

Signature (Dean/Principal): _______________________

Date: 08-08-2023

Form TH-4

National University of Sciences & Technology (NUST)

MASTER'S THESIS WORK

We hereby recommend that the dissertation prepared under our supervision by: Danial Iltaf (00000317724) Titled: System Identification of Vibrational System using GMR Sensor be accepted in partial fulfillment of the requirements for the award of MS in Mechanical Engineering degree.

Examination Committee Members

1. Name: Riaz Ahmed Mufti Signature:

2. Name: Jawad Aslam Signature:

3. Name: Rehan Zahid Signature:

Supervisor: Mian Ashfaq Ali Signature:

Date: 08 - Aug - 2023

Head of Department

08 - Aug - 2023

Date

COUNTERSINGED

08 - Aug - 2023

Date

Dean/Principal

Declaration

I certify that this research work titled "*Smart Concrete 3D printer Extruder Design and Prototyping"* is my own work. The work has not been presented elsewhere for assessment. The material that has been used from other sources it has been properly acknowledged / referred.

Signature of Student

Danial Iltaf

2019-NUST-MS-Mech-317724

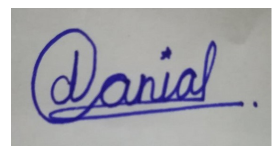

Language Correctness Certificate

This thesis has been read by an English expert and is free of typing, syntax, semantic, grammatical, and spelling mistakes. Thesis is also according to the format given by the university.

Signature of Student

Danial Iltaf

2019-NUST-MS-Mech-317724

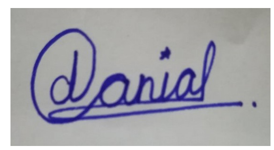

Signature of Supervisor

Proposed Certificate for Plagiarism

It is certified that MS Thesis Titled **System Identification of Vibrational System using GMR Sensor** by **Danial Iltaf** has been examined by me. I undertake the follows:

a. Thesis has significant new work/knowledge as compared already published or are under consideration to be published elsewhere. No sentence, equation, diagram, table, paragraph or section has been copied verbatim from previous work unless it is placed under quotation marks and duly referenced.
b. The work presented is original and own work of the author (i.e. there is no plagiarism). No ideas, processes, results or words of others have been presented as Author own work.
c. There is no fabrication of data or results which have been compiled/analyzed.
d. There is no falsification by manipulating research materials, equipment or processes, or changing or omitting data or results such that the research is not accurately represented in the research record.
e. The thesis has been checked using TURNITIN (copy of originality report attached) and found within limits as per HEC plagiarism Policy and instructions issued from time to time.

Name & Signature of Supervisor

Dr. Mian Ashfaq Ali

Signature: 

Copyright Statement

- Copyright in text of this thesis rests with the student author. Copies (by any process) either in full, or of extracts, may be made only in accordance with instructions given by the author and lodged in the Library of NUST School of Mechanical & Manufacturing Engineering (SMME). Details may be obtained by the Librarian. This page must form part of any such copies made. Further copies (by any process) may not be made without the permission (in writing) of the author.
- The ownership of any intellectual property rights which may be described in this thesis is vested in NUST School of Mechanical & Manufacturing Engineering, subject to any prior agreement to the contrary, and may not be made available for use by third parties without the written permission of the SMME, which will prescribe the terms and conditions of any such agreement.
- Further information on the conditions under which disclosures and exploitation may take place is available from the Library of NUST School of Mechanical & Manufacturing Engineering, Islamabad.

Acknowledgements

I am thankful to my Creator Allah Subhana-Watala to have guided me throughout this work at every step and for every new thought which Your setup in my mind to improve it. Indeed, I could have done nothing without Your priceless help and guidance. Whosoever helped me throughout the course of my thesis, whether my parents or any other individual was Your will, so indeed none be worthy of praise but You.

I am profusely thankful to my beloved parents who raised me when I was not capable of walking and continued to support me throughout in every department of my life.

I would also like to express special thanks to my supervisor **DR. Mian Ashfaq Ali** for his help throughout my thesis. He has been exceptionally helpful throughout my journey & it is because of his continuous help and guidance that I am able complete this project in time. He is a kind soul and a guide for life.

I would also like to pay special thanks to **Dr. Riaz Ahmad Mufti, Dr. Jawad Aslam, Dr. Rehan Zahid, Dr. Usman Bhutta** and **Fazal Badshah** for his tremendous support and cooperation. Each time I got stuck in something; he came up with the solution. Without his help I wouldn't have been able to complete my thesis. I appreciate his patience and guidance throughout the whole thesis.

Finally, I would also like to express my special thanks to **Aaras Ahmed Bhatti** for his help in the lab, in the hostel, in the grounds, in the cafe and nearly all other aspects of life. He has a knack for interfering in other people life and make it better for them. I am indebted to him and wish him best of luck in his life. Also, I would like to thanks all the other fellow students in the for their help especially **Muhammad Umais Qamar, Faheem Abbas, Haseeb Adil, Umar Farooq, Qasim Sajid, Atta ur rehman** and all the senior students for a great environment of the lab.

Dedicated to my exceptional parents and adored sibling whose tremendous support and cooperation led me to this wonderful accomplishment.

Abstract

In this study, GMR Sensor AAH002-02E is used along with a standard permanent (Neodymium) magnet, Response of sensor is observed along a linear range and is calibrated for this standard magnet. GMR sensors have the ability to measure vibration without contact as they can detect variation induced in magnetic field. So, these sensors are widely used for vibration detection and measurement. Cantilever beam type system was used and an initial disturbance was applied at the free end of this cantilever beam which introduced vibration in beam. The data is collected through DAQ card. Initially the signal is in voltage vs time format which is then converted to distance vs time to visualize the motion.

Key Words: GMR, SI, GMR Sensor, Vibration measurement, Analog Magnetic Sensor

Table of Contents

List of Figures

List of Tables

Chapter 01

Introduction to System Identification

Inferring models from observation and studying their properties is really what science is all about. The models ("hypotheses." "Laws of nature," "paradigms," etc.) may be of more or less formal character, but they have the basic feature that they attempt to link observations together into some pattern. System identification deals with the problem of building mathematical models of dynamical systems based on observed data from the system. The subject is thus part of basic scientific methodology, and since dynamical systems are abundant in our environment, the techniques of system identification have a wide application area.

1.1 Brief History

The early work in system identification was developed by the statistics and time series communities. It has its roots in the work of Gauss (1809) and Fisher (1912) and the theory of stochastic processes but the state-space era started in 1960 with Kalman’s key papers. Kalman developed a model-based theory for prediction, filtering and control. A Kalman filter is an optimal estimator i.e., it infers parameters of interest from indirect, inaccurate and uncertain observations. It is recursive so that new measurements can be processed as they arrive. (Batch processing where all data must be present). As a result

- Kalman filter replaces Wiener filter
- Pole placement and LQG control
- Applications initially in areas where good models are available (aerospace, mechanical, electrical systems)

This caused a growing pressure to apply these modern techniques to areas where models are not available from physics. As a result, the need for System Identification became ever more evident.

1.2 System

To understand system identification, we first need to understand what is a system. To put it simply, a system is basically an object where variables of different kind interact to produce an observable signal. This observable signal that we get at the end is called “output of the system” or simply “output”, this product of the system is of interest for us. The output of the system is affected by external stimuli usually controlled by the observer and is called “Input of the system” or simply “input”. Other signals that are unwanted in our system and effect our output and is not in control of the observer is called disturbance. Some of these disturbances can be directly measured while other can only be observed by their influence on the output signal. The disturbances that can be measured directly are of little consideration because they can be easily filtered out or catered for. Figure below shows a system with both measured and unmeasured disturbances.

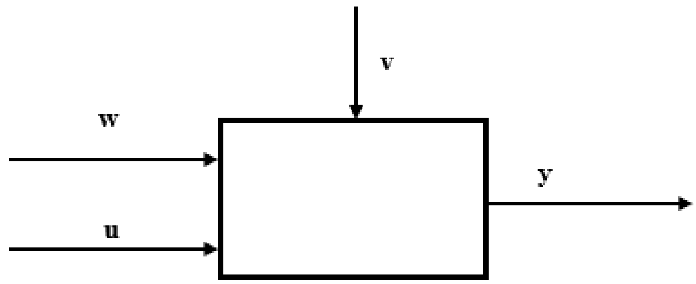

Figure 1: A Dynamic System

Figure shows a system with output ‘y’, input ‘u’, measured disturbance ‘w’ and unmeasured disturbance ‘v’. The concept of a system is broad and it plays a vital role in modern science. Most of the modern-day problems are solved in a system-oriented framework.

1.3 Identification

Identification is the task of constructing a dynamic system that can predict the output of this dynamic system. Just like there are different kind of disturbances, there are also different kind of systems. Some systems have user defined inputs and noise while others are only driven by disturbances. The model developed by the system identification is supposed to deal with all these different kinds of system.

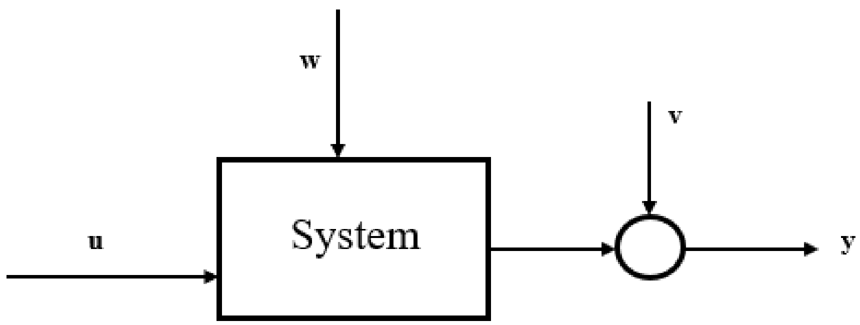

Figure 2: System driven by Input and noise

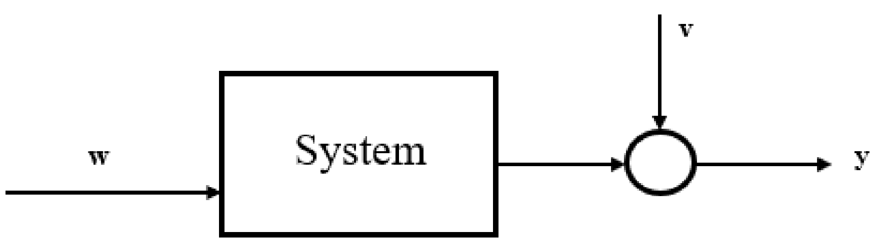

Figure 3: System driven by noise only

1.4 System Identification in Engineering

1965, Identification techniques made their debut in engineering when Ho and Kalman constructed linear state space variable method from input-output data which gave birth to realization theory and subsequently 'subspace identification', at the same time Astrom and Bohlin's Numerical identification of linear dynamic systems from normal operating records gave birth to 'Prediction Error Identification'. Since then, multiple methods have been developed to help with the process of SI, but most prominent of these methods remain **State Space method** and **Input/Output (I/O)** method until 1975. State space model is based on Hankel matrix factorization. This method is easy but not optimal and there is no need for parametrization. Input/Output method is based on minimization of prediction error criterion. This method is slower but much more optimal. This method requires choice of model structure and allows characterization of variance errors through Fisher information matrix. After 1975, PE technique took over mainly because of increased computational speed which catered for the time needed for it. But again in 1990's Hankel matrix approach (subspace state-space method) re-emerged.

A lot of work has been done on system identification but the major setback still remains the search for the best model structure. Modeling and identification cost for any advanced control design is roughly around 50 to 75% of the total projects.

Chapter 02

Literature Review

GMR was first discovered in 1986 after that it has been very effective in the field of physics and engineering. Many researchers are working on GMR and countless publication have been made in the field. Some of the researches that were vital in the field are mentioned here.

2.1 Vibration Detector based on GMR Sensors

In 2007, a journal was published by 'Polytechnical University of Valencia, SPAIN', in which they introduced a new way to measure the vibrations. Up until that, vibrations were usually sensed by their displacement, velocity or acceleration but they measured vibration by the amount the body introduces the magnetic field variations. They used SS501 GMR magnetic sensor for this purpose. The idea behind was, Earth's magnetic field is constant over a wide area but small ferromagnetic pieces can disturb this field by some amount which is detectable by GMR sensor. They build an array formation of sensors detecting field over all three axes from the senso. The block diagram showing the array is shown underneath.

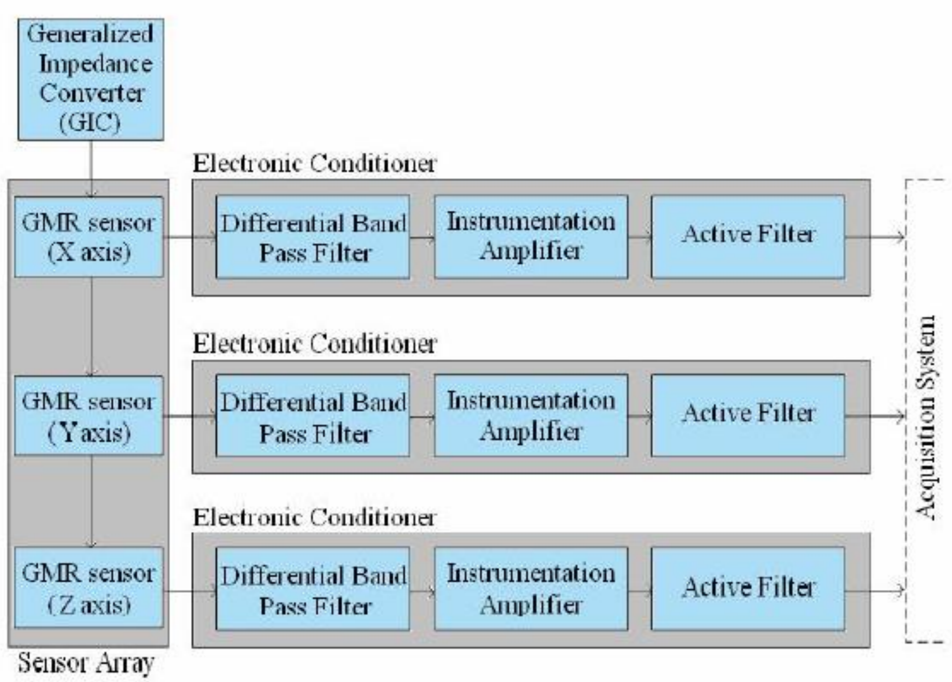

Figure 4: Block diagram of the vibration detector architecture

They took a small drilling machine and tested their setup to measure the rotation speed and disturbance caused by it in various scenarios over all 3 axes. The experiment was successful and the GMR sensor was capable to detect the small perturbations in earth's magnetic field caused by the drill machine.

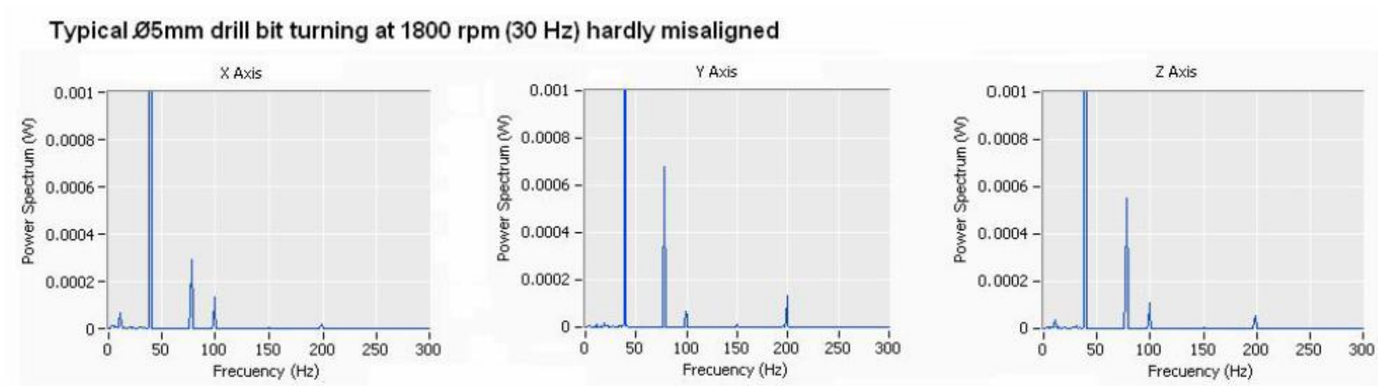

Figure 5: Power spectrum at varying frequency for hardly misaligned drill

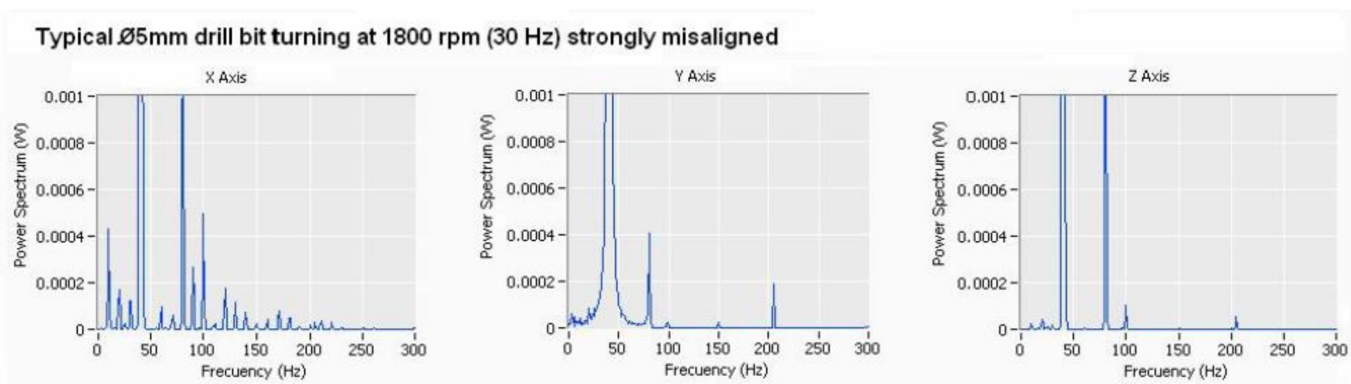

Figure 6: Power spectrum at varying frequency for strongly misaligned drill

Drill bit was rotating 2cm above the sensor. In the 2nd case it is kept intentionally misaligned which reveals several differences in its signature spectrum. In the end, it is concluded that GMR sensors are sensitive enough to detect vibrations even in small machines like drill machine. This is quite appealing to the us as sensor has small power consumption and low manufacturing cost and can be easily used in portable systems.

2.2 GMR sensor for seismic exploration

In 2019, research was conducted on the effect of vibration sensors based on GMR effect in College of Instrumentation and Electrical Engineering, Jilin University, Changchun 130061, China. GMR sensor chip SS501 A was used in the research. The sensor was calibrated using a vibration table and the effective bandwidth range was noted between 6 Hz - 254.2 Hz.

Figure 7: Experimental environment

The experiment indicated that the sensor has a wide bandwidth with a stable output. Experiment was conducted the output of the sensor for seismic vibration was compared with a moving coil geophone and it can be seen that the signal obtained by the GMR sensor is higher than that of a moving coil geophone.

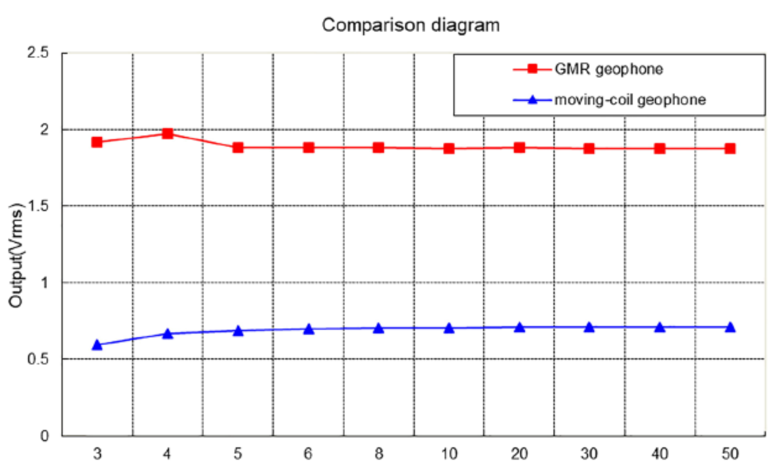

Figure 8: Comparison of a GMR sensor and moving coil geophone output

2.3 GMR Magnetic field measurement at increasing Temperature Conditions

In 2020, School of Engineering, London South Bank University, London, UK, research was conducted to study the thermal stability of the GMR sensors. A commercial GMR sensor was used to measure the magnetic field response of the system. The worked aimed to act as fully operational evidence of the application, keeping in mind the standard mode of operation and to improve the sensitivity. NVE AA002-02 sensor was used for this experiment. 6 tests were conducted starting from room temperature and then increasing 10 ^{0}C for every experiment. The vibration setup they used and the Variation in sensor output with respect to the temperature is shown below,

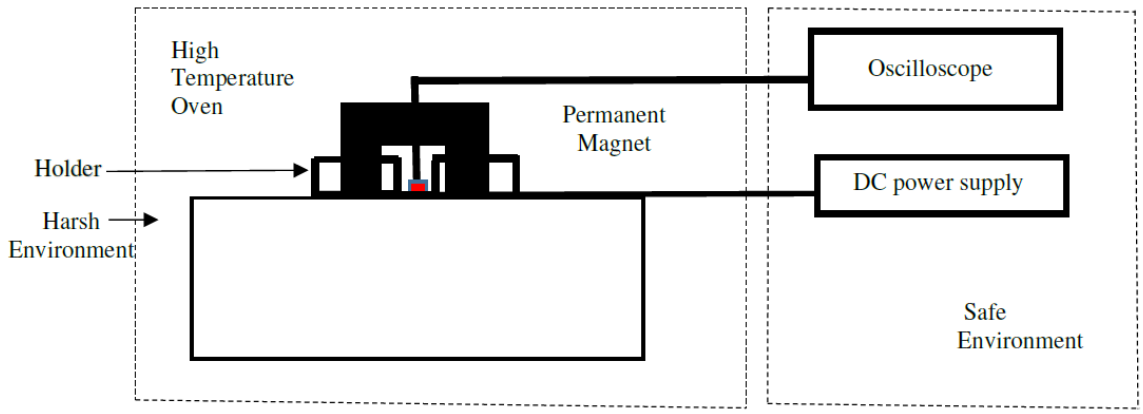

Figure 9: Measurement system

Figure 10: Actual setup using GMR sensor

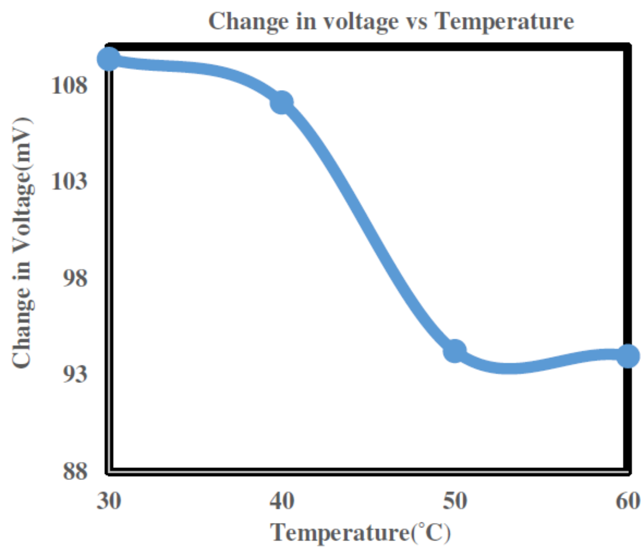

Figure 11: Voltage change vs Temperature

Evidentially the sensor catalog also provided a temperature dependent survey for the AA002-02 sensor and the output is shown below,

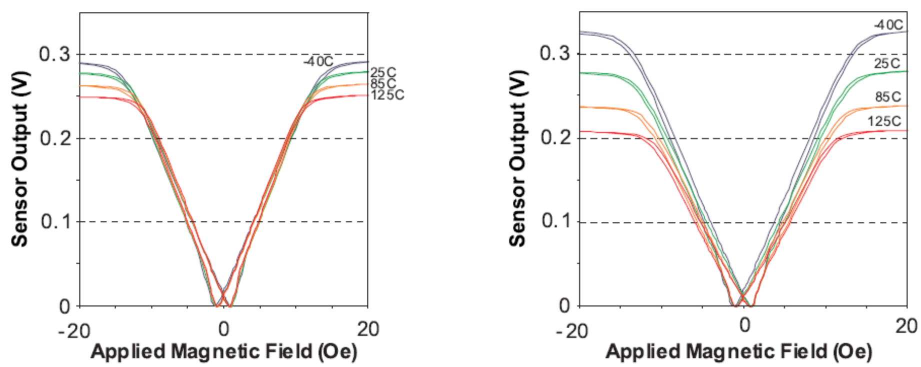

Figure 12: Sensor response at constant current drive and fixed voltage supply

At the end, it can be concluded that, GMR sensor AAH002-02 sensor has an excellent temperature stability especially with a constant current drive. It can precisely work at high temperatures up to 80 degrees as per this study meanwhile the sensor catalog claims it has a temperature stability until 150 degrees.

2.4 Detecting small defects in conductive thin metallic layers using GMR sensor

In this research, injected AC current techniques and GMR are used to detect defects in conductive thin metallic layers. The defects were the size of a few hundred micrometers. AC current is injected in between two metallic layers and the perturbations that appear due to a defect are detected using the GMR sensor. A silicon wafer with copper metallization of few micrometers in thickness was used. A 2.5mm long scratch was created on the sheet with a width of 0.2mm. Two measurements were conducted for this setup, one with the sensitive axis parallel to the scratch and one with sensitive axis perpendicular to the scratch. Defect was successfully detected in both cases with a signal to noise ratio (SNR) way over 3 which is the minimum required.

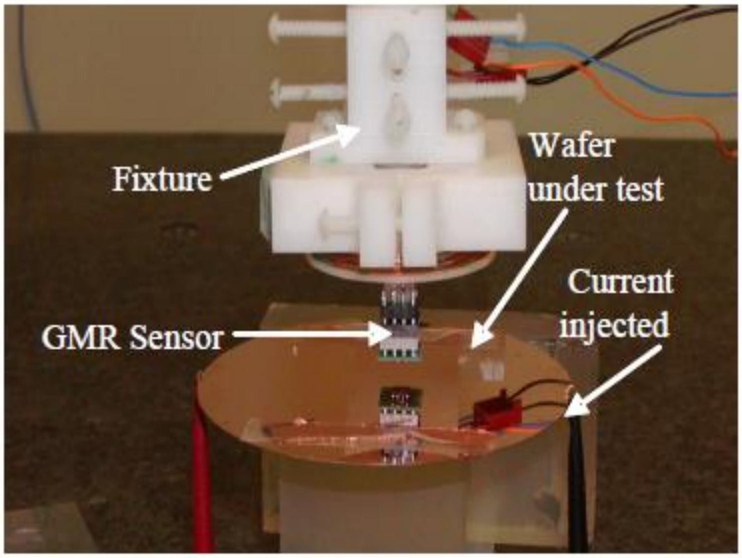

Figure 13: Experimental setup

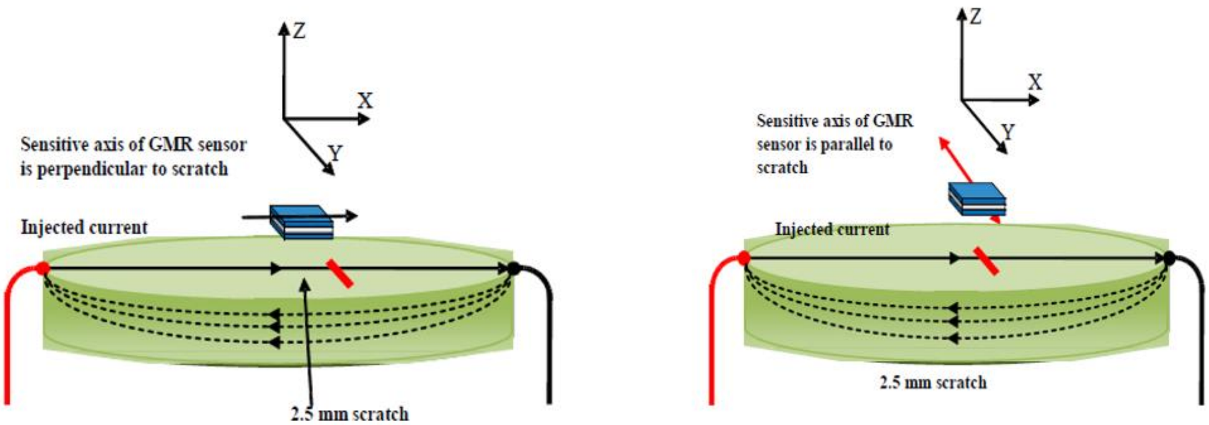

Figure 14: Setup with sensitive axis perpendicular to the scratch (Left) and parallel to the scratch (Right)

Results obtained from these setups are shown below

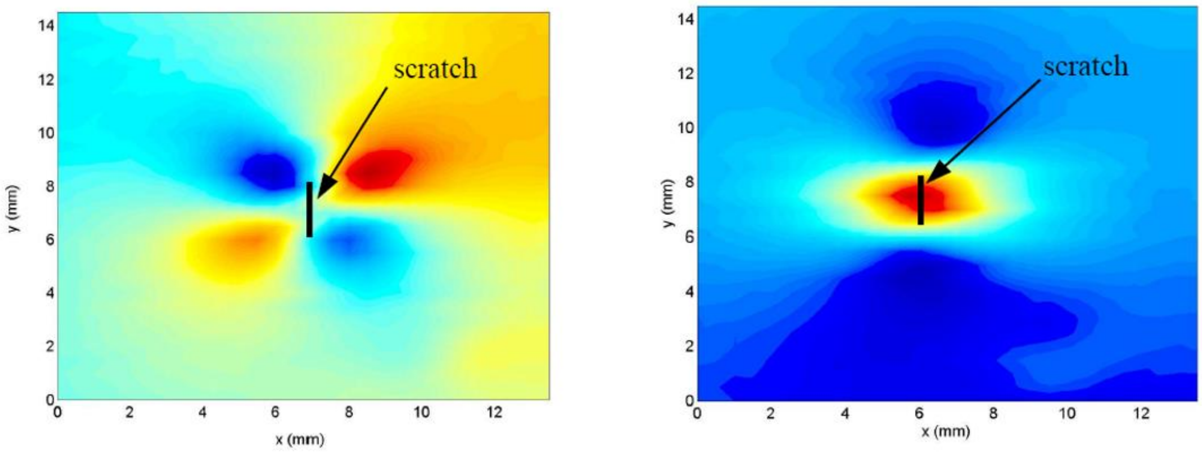

Figure 16: Map obtained from scanning the sensor over a copper wafer where the sensitive axis was perpendicular to the scratch (Left) and parallel to the scratch (Right)

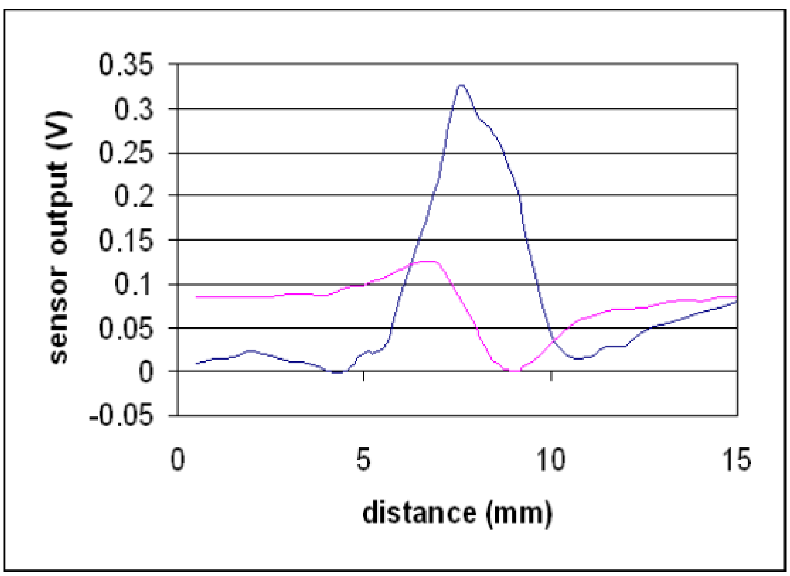

Figure 15: Comparison of signal output by changing orientation of sensitive axis

As shown in the graph above, when the sensitive axis of the sensor was parallel to the scratch, a voltage output as high as 0.33V was obtained which has a SNR ratio of 66 but even when the sensitive axis was perpendicular the SNR remained at 26.

It is concluded in this study that GMR sensor can be used to defect even small defects in conductive thin films. By using another sensor which has a better cross axis sensitivity such as Aah002-02e, we can improve our signal strength even further.

2.5 GMR sensor in medical

GMR sensor are also being used in medical setups. One such example is the research of Nithyaselvakumari in 2020 in which she attempted 'Preclinical diagnosis of asthma with GMR sensor and RADWT algorithm'. Asthma is a very common chronic disease which cause difficulty in breathing. Even though it's a very common disease the early diagnosis is always a problem because its symptoms are often confused with common cold. In this paper a noninvasive method to detect asthma in early stage is proposed.

The lungs are blocked because of mucus forming in the lungs. The mucus is a combination of water, potassium chloride, proteins, electrolytes, calcium, phosphate, sodium bicarbonate, magnesium and lipids. The mucus causes varying magnetic field either by accumulating or by dynamic flow. The magnetic emission directly proportional to this accumulation or dynamic flow. Normal and constricted air lungs is shown below

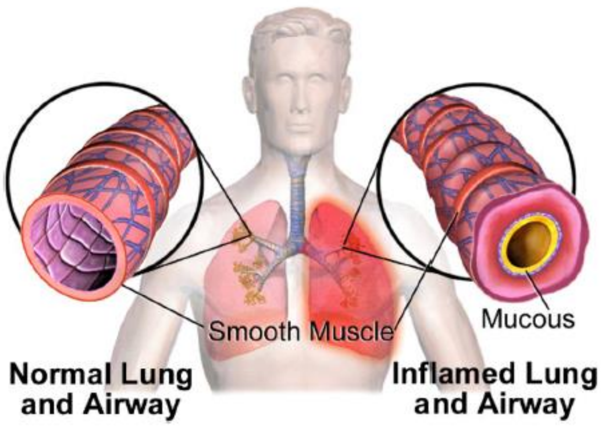

Figure 17: Normal and constricted air lungs

Figure 18: Spin tropic GMR sensor

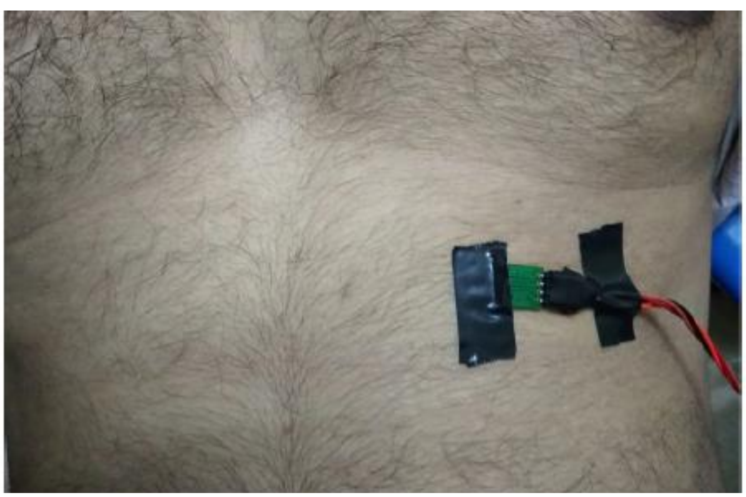

Figure 19: GMR sensor placed on lung for Asthma detection

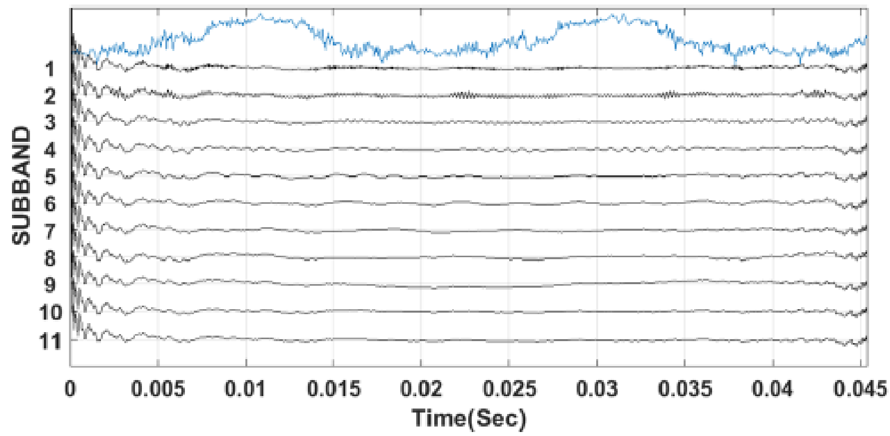

Figure 20: RADWT decomposition of a normal person mucus bio magnetic signal

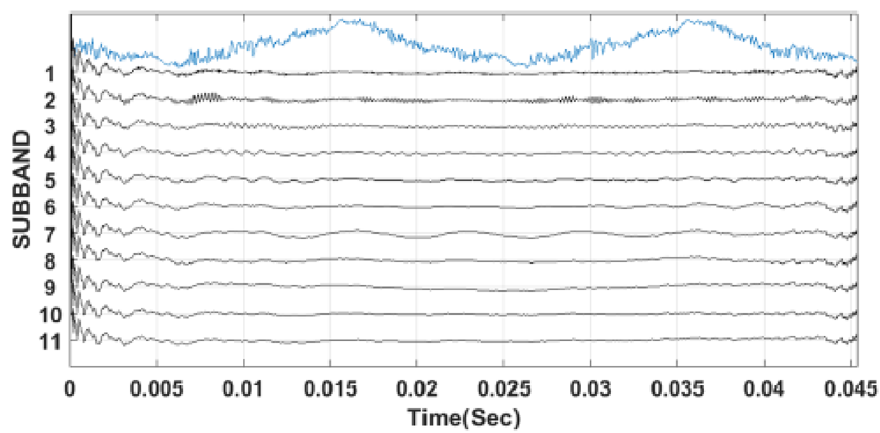

Figure 21: RADWT decomposition of an intermittent asthma person mucus bio magnetic signal

The patient was having wheezing condition 2-3 times a week. GMR sensor captured the mucus magnetism which shows influence of accumulated mucus on subband 2 and 3.

Chapter 03

Vibrational Systems

Vibration is a mechanical phenomenon in which oscillations occur around an equilibrium point. It occurs when a body is displaced from its equilibrium position. Vibrations are sometimes desirable for example when we want to produce sound, basically all music instruments and working on the basis of this vibration. On the other hand, in some applications it is very undesirable. For example, vibrations of a particular frequency can indicate a fault in a system or component, it can be commonly observed in automobiles. In any case, it is essential to sense these vibrations as they are prevalent in essentially every industry.

3.1 Natural and Damped Vibrations

Vibrations of mechanical systems can be classified most simply in two characteristics i.e. If this vibration is free or forced and the amount of damping in the system. A **free vibration** is the one in which a system is displaced once but after that there is no external force that keeps the body in motion. This vibration is caused by an initial displacement and then it is free to oscillate at its natural frequency. An example of free vibration is plucked guitar string. A **Forced vibration** is the one when an alternating force or motion is applied to a system. This external force is being applied constantly and the body's vibrating frequency and amplitude is controlled by this force. Example of this type of vibration is shaking of a building due to an earthquake. The amplitude and frequency of the vibrations are determined by the earthquake and not the building. In the most general case, a vibrating system can be modeled by a second order linear system with mass M, damping coefficient D, stiffness K, and external force F.

$$M \frac{d^2x}{dt} + D\frac{dx}{dt} + Kx = F \tag{3.1}$$

Damping is the amount of friction that acts on the system to dissipate the energy of the system. A system can be categorized as undamped, underdamped, over damped or critically damped. Undamped system keeps on oscillating indefinitely at a constant amplitude. Under damped system will oscillate with a decreasing amplitude until it reaches equilibrium. Critically damped and over damped system will both come to equilibrium without oscillating, the difference between them is that the critically damped system will take the least amount of time to reach equilibrium. The amount of damping in a system is best described by the damping ratio, ζ. The damping ratio is given by:

$$\zeta = \frac{D}{2\sqrt{KM}} \tag{3.2}$$

This ratio varies form undamped ($\zeta = 0$), underdamped ($\zeta < 1$), critically-damped ($\zeta = 1$), and overdamped ($\zeta > 1$). Effect oof damping on vibration is shown in the figure below.

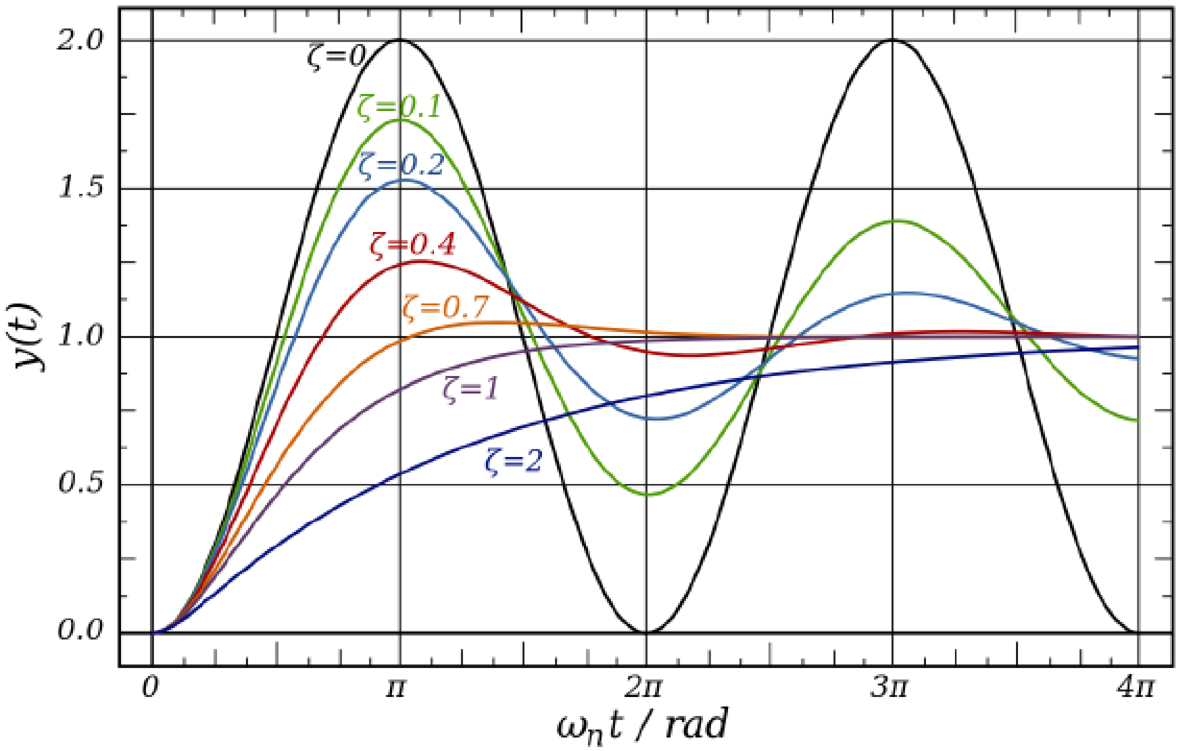

Figure 22: Effect of damping on Vibrations

It can be seen from the figure that as ζ increases from zero, the oscillation amplitude decreases at a faster rate. If ζ goes above one, the signal does not overshoot, but takes longer to reach equilibrium than the critically-damped case ($\zeta = 1$).

Equation (3.1) can be rewritten to include ωn and ζ as follows:

$$\frac{d^2x}{dt} + 2\zeta\omega_n\frac{dx}{dt} + {\omega_n}^2x = F \tag{3.3}$$

In addition to altering the amplitude of vibration, the damping ratio also shifts the frequency of vibration. The new frequency is called the damped natural frequency:

$$\omega_d = \omega_n\sqrt{1-\zeta^2} \tag{3.4}$$

3.2 Degree of Freedom

Degree of freedom is the number of directions in which a particle can move freely or the total number of coordinates required to describe completely the position and configuration of the system. These localized coordinates that are required to fully describe the motion of a system are known as generalized coordinates, they can either be Cartesian or non-Cartesian coordinates. System that only need one coordinate system to define the whole system have degree of freedom equals to 1. Examples of single degree of freedom are as follows

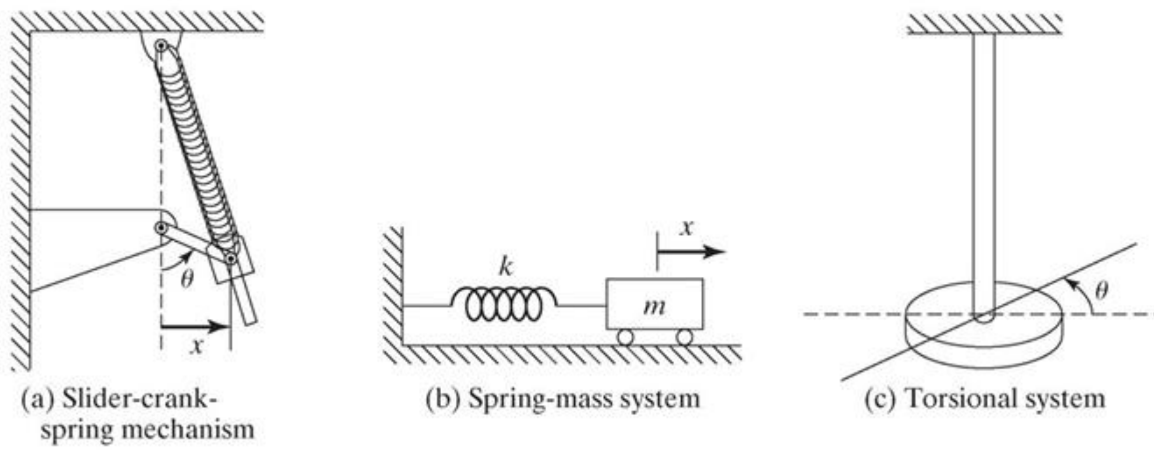

Figure 23: Examples of single degree of freedom systems

Systems can also have degree of freedom other than one. Examples of multiple degree of freedom system are shown below.

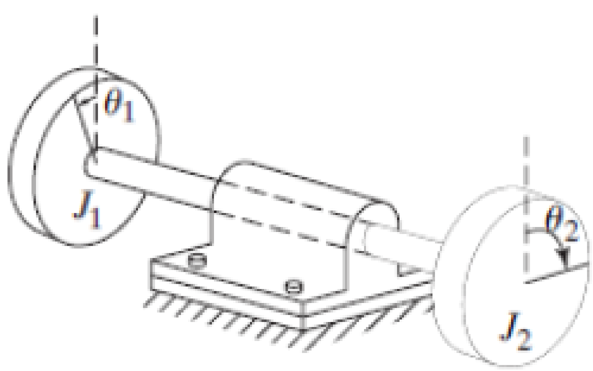

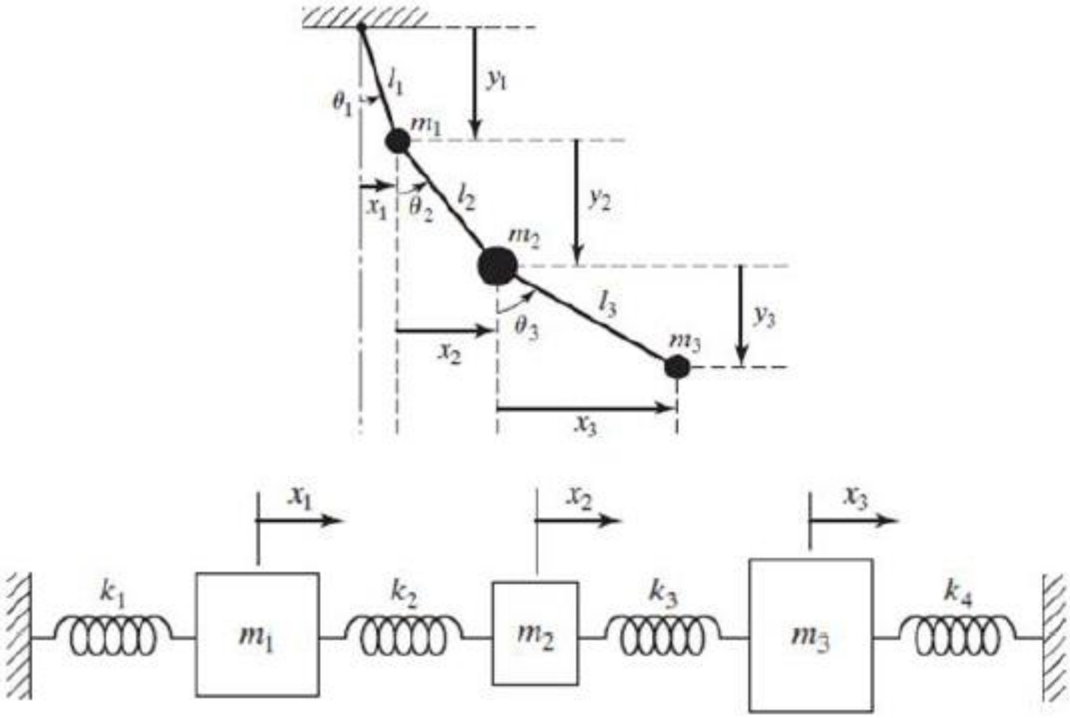

Figure 25: 3rd degree of freedom system

3.3 Linear and non-linear system:

All real systems are non-linear up to some extent and are dealt with nonlinear differential equations. System will be called linear if all of its components e.g., mass, spring and damper etc. in a mass spring damper system behave linearly. Most of these non-linear systems can be made linear by restricting its range and smoothing out the non-linearities. Linear system is simple and easy to deal with. A linear system can be represented in the form of $\dot{x} = Ax$, where x represents states and A itself represents the system matrix. However, if any of the components starts behaving non-linearly then the whole system will be considered as non-linear.

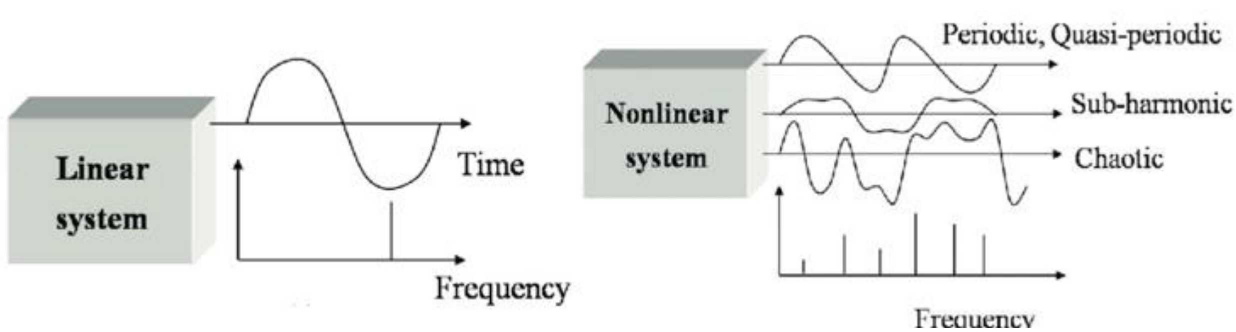

Figure 26: Linear and non-linear system

Chapter 04

GMR

Giant magnetoresistance (GMR) is a quantum mechanical magnetoresistance effect observed in multilayers composed of alternating ferromagnetic and non-magnetic conductive layers. In 2007, Albert Fert and Peter Grünberg received the Nobel prize in Physics for their discovery of GMR. They observed that, depending upon the magnetization of adjacent ferromagnetic layers (parallel or anti parallel) a very significant change in resistance takes place. For parallel alignment, the overall resistance is relatively low. For antiparallel alignment, overall resistance is relatively very high. By applying an external magnetic field, the direction of magnetization can be controlled. The effect takes place because of electron scattering dependance on spin orientation.

GMR effect found its main use as magnetic field sensors. These are used to read data on hard disk drives, microelectromechanical systems (MEMS) and other devices. Magneto-resistive random-access memory (MRAM) uses GMR multilayer structure as cells that store one bit of information.

Imagine a non-magnetic layer sandwiched in two magnetic layers. Take a look at the picture below

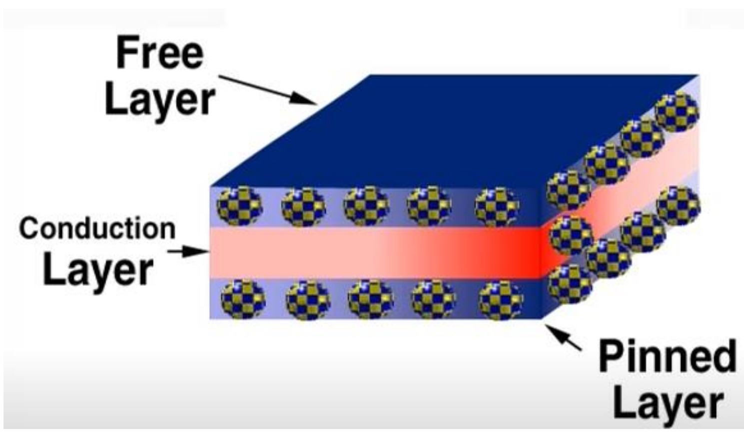

Figure 27: GMR Phenomenon

The balls represent electrons, the middle layer is non-magnetic conduction layer and it needs to be thinner than the mean free path of conduction electrons which is only a few nanometers. The top layer is called the free layer because its electron spins are free to change the direction of orientation. The bottom layer is the pinned layer or reference layer because its spin orientation is fixed when the device is made. In this state the electrons spin in opposite directions in the top and bottom layers which causes the electrons in the middle to scatter increasing resistance. But when a magnetic field is applied to this system as shown in the figure below, its resistance drops significantly.

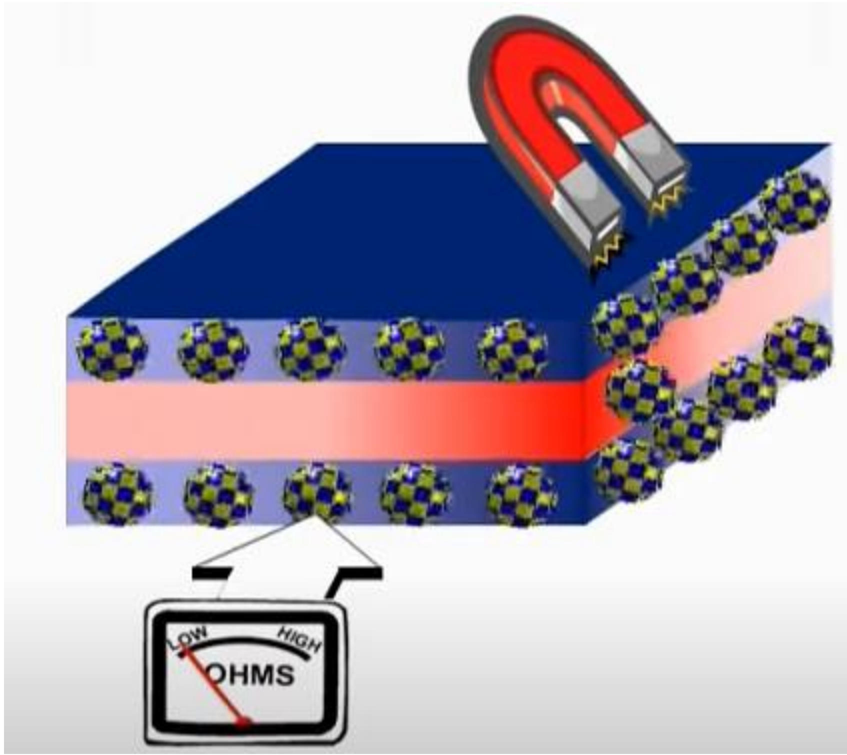

Figure 28: Low resistance of GMR after applying magnetic field

When a magnetic field is applied, electron spins in the free layer switch direction, conduction electrons scatter less and as a result a significant resistance drop takes place. The magic of GMR is turning the esoteric property of electron spin into resistance which can be used by conventional electronics.

4.1 History

GMR sensor was discovered in 1998 by Peter Grünberg of Forschungszentrum Jülich, Germany and Albert Fert of the University of Paris-Sud, France, independently. Considering the significance of their discovery they were awarded a Nobel prize in Physics in 2007.

Grünberg and Fert studied the electrical resistance of various structures including ferromagnetic and non-ferromagnetic materials. Fert work was on multilayer structures. The Fert group used (001) Fe/ (001) Cr superlattices wherein the Fe and Cr layers were deposited in a high vacuum on a (001) GaAs substrate kept at 20 °C and the magnetoresistance measurements were taken at low temperature (typically 4.2 K). Meanwhile, in 1986 Grünberg discovered the antiferromagnetic exchange interaction in Fe/Cr films. He worked on multilayers of Fe and Cr on (110) GaAs at room temperature.

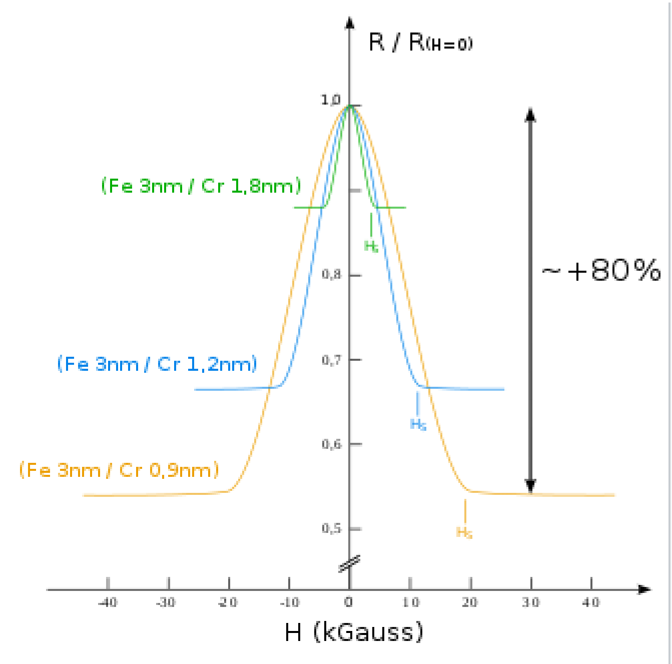

Figure 29: The founding results of Albert Fert and Peter Grünberg (1988): change in the resistance of Fe/Cr superlattices at 4.2 K in external magnetic field. The arrow to the right shows maximum r esistance change. Hs is saturation field.

4.2 Materials and experimental data

GMR phenomenon is exhibited by many materials, and the most common are the following:

- FeCr
- $Co_{10}Cu_{90}$: δ_H = 40% at room temperature
- [110] Co_{95}: Fe_5: /Cu: δ_H = 110% at room temperature

Magnetoresistance depends on many factors such as geometry, temperature, thickness of both ferromagnetic and non-magnetic layers. Using a cobalt layer of 1.5 nm at 4.2K temperature, by increasing the thickness from 1 to 10 mm decreases the δ_H from 80 to 10%. Meanwhile the best δ_H was observed for thickness 2.5nm. When the temperature of a Co(1.2 nm)/Cu(1.1 nm) superlattice was increased from near zero to 300K, its δ_H decreased from 40 to 20% for current in plane geometry and from 100 to 55% in current perpendicular to plane geometry.

4.3 Types of GMR

Classification of GMR is done based on the type of device that exhibits the effect

4.3.1 Multilayer

In multilayer GMR, two or more magnetic layers are separated by an insulating layer. Insulating layer in non-magnetic and is generally very thin, up to approx. 1nm. Ferrite is often used as magnetic layer whereas chrome is used as insulating layer. At certain thickness, the coupling between adjacent ferromagnetic layers becomes antiferromagnetic, which makes it preferable to align the magnetization of layers in anti-parallel direction. This could result in 10% change in electrical resistance.

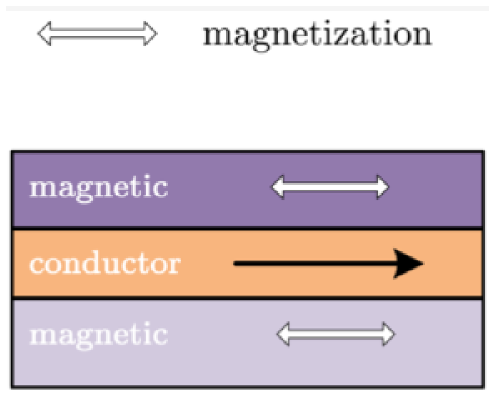

Figure 30: Multilayer structure

4.3.2 Spin Valve

In spin valve GMR, two magnetic layers are separated by an insulating layer. Insulating layer in non-magnetic and is very thin, up to approx. 3nm. Copper and an alloy of Nickel and iron are often used as in spin valve GMR. Spin valve GMR is the most useful sort for hard drives

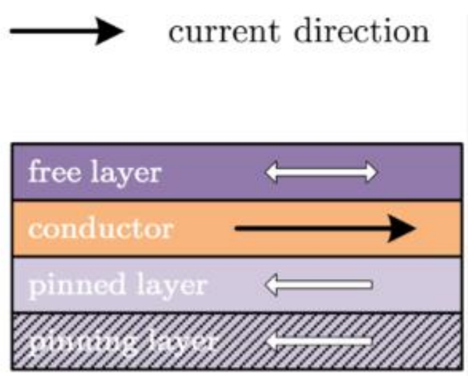

Figure 31: Spin Valve GMR

4.3.3 Granular GMR

Granular GMR is the effect that occurs in solid precipitate of magnetic material in a non-magnetic matrix. It has only been observed in copper containing grains of cobalt. The reason is copper and cobalt are immiscible. Their properties strongly depend upon annealing temperature and measurement. They can also exhibit inverse GMR.

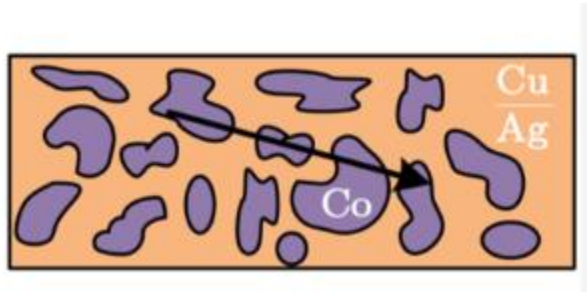

Figure 32: Granular GMR

Chapter 05

GMR Sensor, Properties, Assembly & Calibration

5.1 Sensor

The sensor used for this study is NVE's AAH002-02e. Main features of this sensor are its high sensitivity, excellent temperature stability and small size. It has a Wheatstone bridge analog output and can work in high temperature conditions up to 150^0 Celsius. Sensor has a Magnetometer configuration and can perform operations in near-zero voltage.

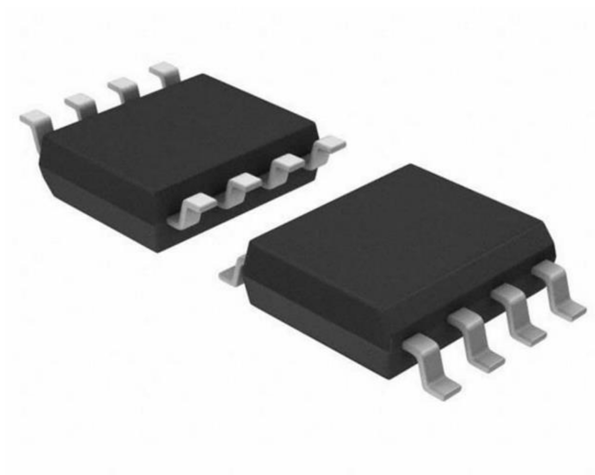

Figure 33: AAH002-02E sensor

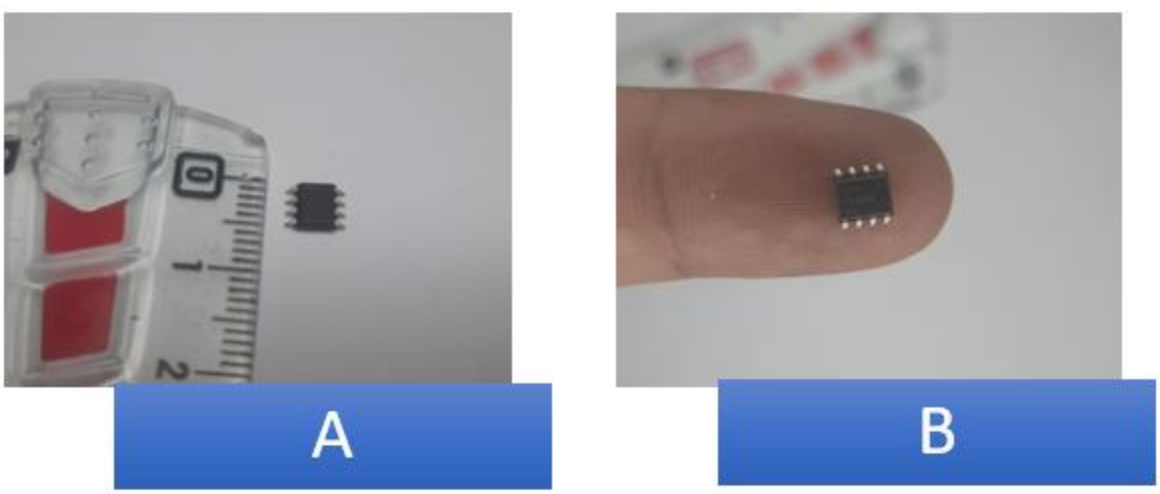

Figure 34: Sensor in real life

5.2 Sensor Properties

The equivalent circuit and idealized transfer functions are shown below.

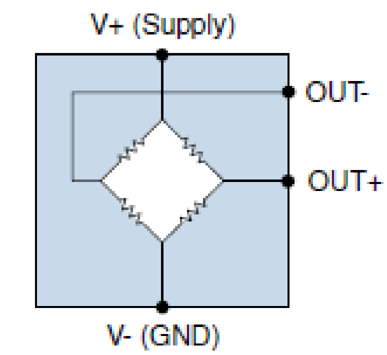

Figure 35: Equivalent Circuit

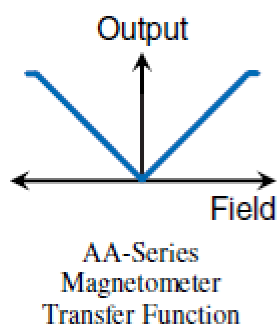

Figure 36: Transfer function of the sensor

NVE's AA series sensors are magnetometers which detect the absolute magnetic field as contrary to AB series which are gradiometers and detect field gradients. The sensors are configured as inherently temperature compensating Wheatstone bridges.

5.2.1 Sensor Operating Range

Operating Specifications of the sensor is shown in the table below

Parameter	Symbol	min	Typ	max	units
Supply voltage	V_{CC}			12	volts
Operating temperature	T			150	°C
Output at max field	V		40		mV/V
Non-Linearity			4		%
Hysterisis			15		%
Frequency Bandwidth	f_{max}			75	KHz
Junction Ambient thermal resistance	Θ_{JA}		240		°C/W
Power Dissipation	P_D		675		mW

Table 1: Operating conditions for AAH002-02e

5.2.2 Sensor properties Comparison

On comparing our GMR sensor with other GMR sensors of NVE, we obtained the following table listing their properties relatively

Parameter	AAxxx/ ABxxx	AAHxxx/ ABHxxx	AAKxxx	AALxxx
Field Sensitivity	High	Very High	Low	High
Operating Field Range	High	Low	Very High	Medium
Hysteresis	Medium	High	Medium	Low
Max. Temperature	High	Very High	Commercial	High

Table 2: Comparison of properties of Various GMR sensors

5.2.3 Direction of Sensitivity

GMR sensor have the direction of sensitivity in the plane of the package. It is a lot more convenient for many applications. Example of these orientation is shown below

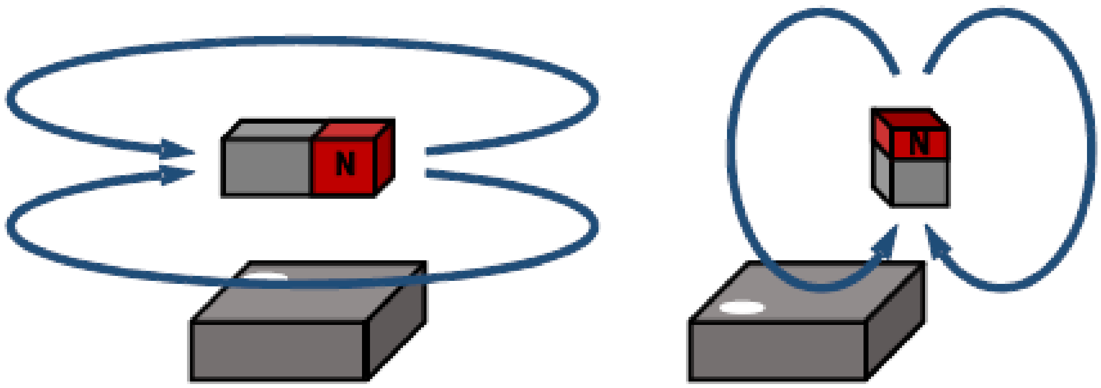

Figure 37: Planar Magnetic Sensitivity

5.2.4 Magnetic field polarity

GMR sensor is 'omni polar'. This indicates that it will be equally sensitive to either magnetic field polarity and the output will always be a positive value.

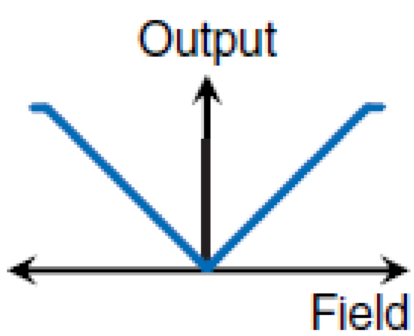

Figure 38: Omni polar response of GMR sensor

5.2.5 Directional Sensitivity

GMR sensor has both, standard and cross axis sensitivity

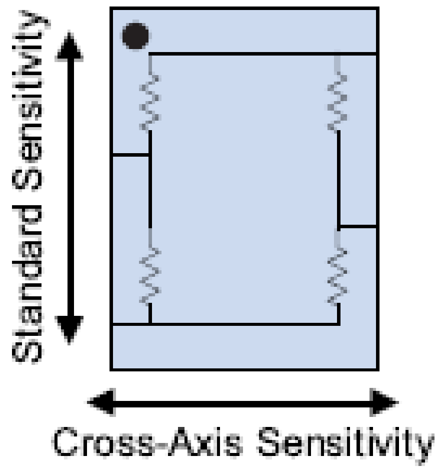

Figure 39: GMR sensor, Standard vs Cross axis sensitivity

5.2.6 Performance graphs

GMR sensor performance at different temperature is shown below

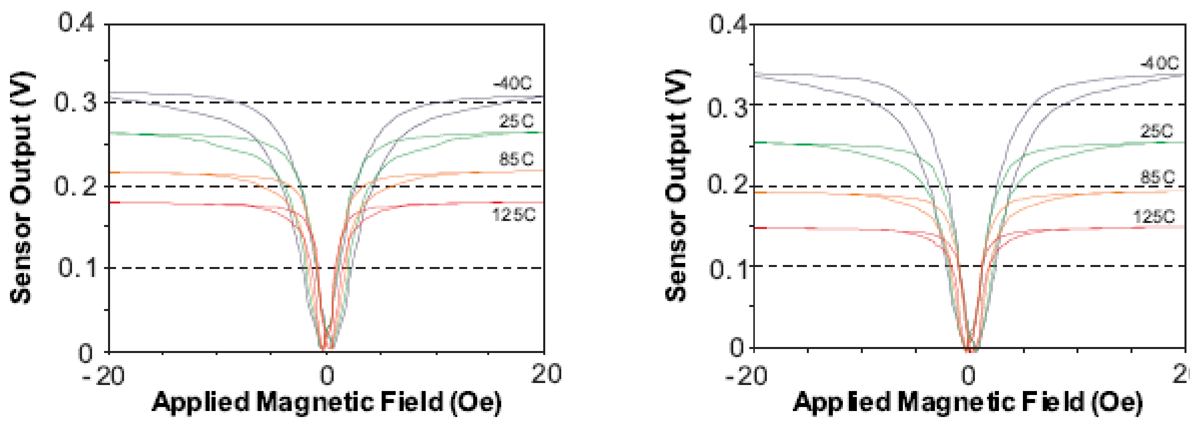

Figure 40: GMR sensor response at different temperatures at constant current drive and constant voltage supply

5.2.7 Part Numbering

GMR sensors naming convention used by NVE is shown below. Just by reading the name you can have a fair amount of information about the sensor.

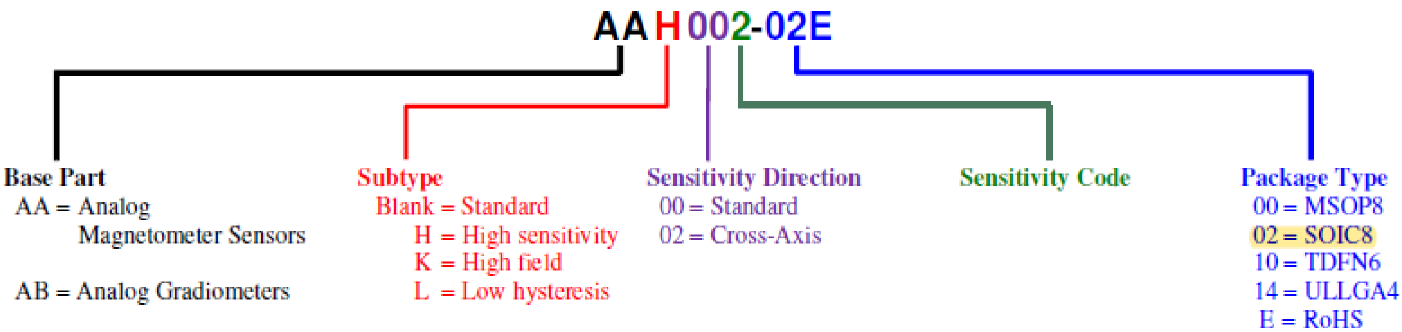

Figure 41: Sensor Naming convention

5.2.8 Pinout

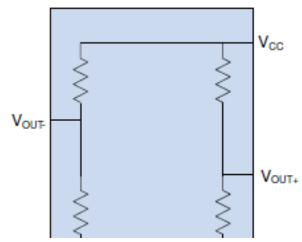

Figure 43: Sensor grey-box layout

Sensitivity						
Standard (AAX00x-xx)			Cross-Axis (AAX02x-xx)			
ULLGA	MSOP/ SOIC	TDFN	MSOP/ SOIC	TDFN	Symbol	Description
3	1	1	5	4	V_{OUT-}	Negative bridge output (decreases with increasing field).
	2 3	2	2 3	2	NC	No internal connection.
4	4	3	4	3	V-/GND	Negative supply or ground.
1	5	4	1	1	V_{OUT+}	Positive bridge output (increases with field).
	6 7	5	6 7	5	NC	No internal connection.
2	8	6	8	6	V+	Positive supply voltage.
		Center Pad		Center Pad	NC	Internally connected to leadframe

Figure 42: Sensor Pinout

5.2.9 Sensor selector Chart

Each GMR sensor used by NVE has a special characteristic to it. To select the sensor that best suits you, you can use this chart and make an informed decision.

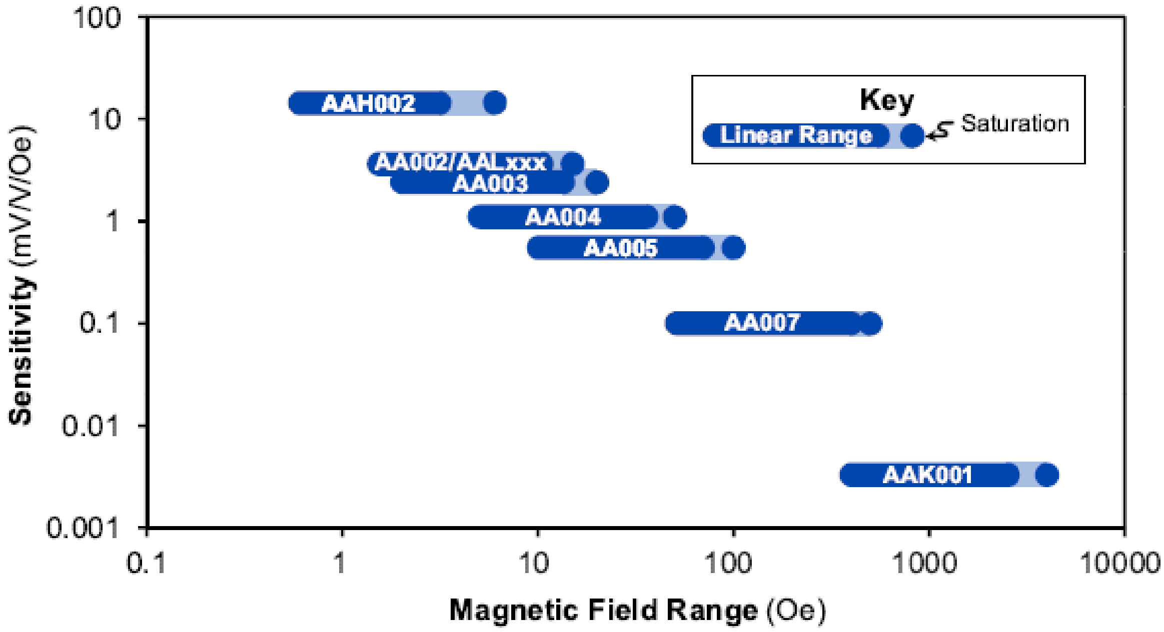

Figure 44: Sensitivity vs magnetic field range chart showing linear range and saturation points for different sensors

5.2.10 Comparative Sensor Specifications

Magnetometers (AA-Series)										
Available Part	Linear Range (|Oe|)		Saturation (|Oe|)	Sensitivity (mV/V-Oe)		Max. Non-linearity (% Uni.)	Max. Hysteresis (% Uni.)	Max. Operating Temp.	Typ. Resistance	Package
	Min.	Max.		Min.	Max.					
AA002-02	1.5	10.5	15	3	4.2	2%	4%	125°C	5 kΩ	SOIC8
AA003-02	2	14	20	2	3.2	2%	4%	125°C	5 kΩ	SOIC8
AA004-00	5	35	50	0.9	1.3	2%	4%	125°C	5 kΩ	MSOP8
AA024-00	5	35	50	0.9	1.3	2%	4%	125°C	5 kΩ	MSOP8 (cross-axis)
AA004-02	5	35	50	0.9	1.3	2%	4%	125°C	5 kΩ	SOIC8
AA005-02	10	70	100	0.45	0.65	2%	4%	125°C	5 kΩ	SOIC8
AA006-00	5	35	50	0.9	1.3	2%	4%	125°C	30 kΩ	MSOP8
AA006-02	5	35	50	0.9	1.3	2%	4%	125°C	30 kΩ	SOIC8
AA007-00	50	450	500	0.08	0.12	2%	4%	125°C	5 kΩ	MSOP8
AAH002-02	0.6	3	6	11	18	4%	15%	150°C	2 kΩ	SOIC8
AAH004-00	1.5	7.5	15	3.2	4.8	4%	15%	150°C	2 kΩ	MSOP8
AAL002-02	1.5	10.5	15	3	4.2	2%	2%	125°C	5.5 kΩ	SOIC8
AAL004-10	1.5	10.5	15	3	4.2	4%	2%	125°C	2.2 kΩ	TDFN6
AAL024-10	1.5	10.5	15	3	4.2	4%	2%	125°C	2.2 kΩ	TDFN6 (cross-axis)
AAK001-14	400	2500	4000	0.0025	0.004	2%	4%	85°C	3.5 kΩ	ULLGA4

Figure 45: A comparative specification chart

5.2.11 Dimensions

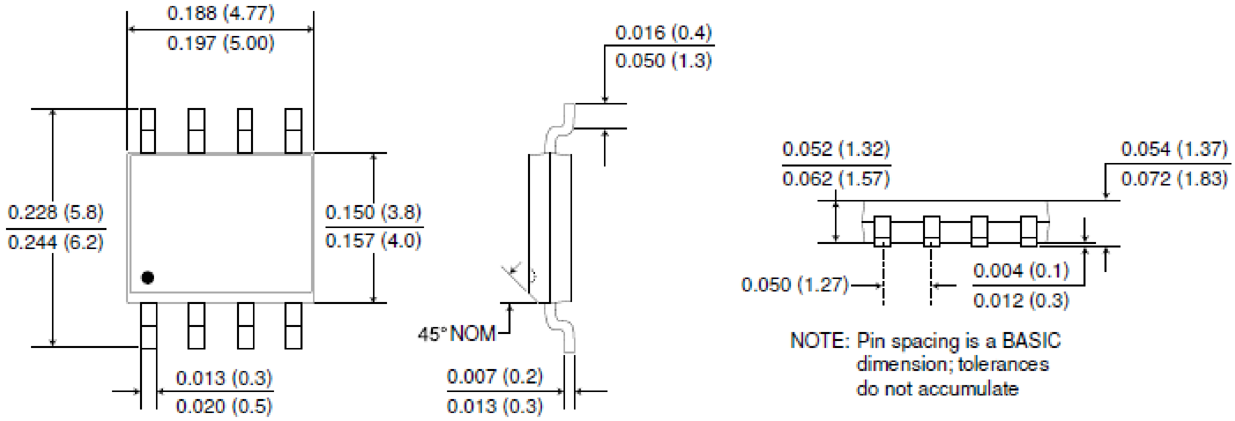

Figure 46: Sensors dimensions

Figure 47: Sensor dimensions validation

5.3 Sensor Working

GMR sensor have two ferromagnetic alloy layers sandwiched around a thin nonmagnetic conductive layer. Due to antiferromagnetic coupling, magnetic moments of ferromagnetic alloys face opposite direction which causes high resistance in the sensor. Copper, which is normally an excellent conductor, is often used as nonmagnetic conductive plate in between these two ferromagnetic layers. Copper has a property that when it is only a few atoms thick it offers a significantly high resistance due to electron scattering. So, in normal state, GMR sensor has high resistance, but when the sensor is exposed to magnetic field, the magnetization of the adjacent layers becomes parallel resulting in significant reduction in resistance. This change is resistance brings forth a change in voltage signal which is of great importance for us.

5.4 Sensor Assembly

5.4.1 Operational Amplifier

An operational amplifier is a DC-coupled high-gain electronic voltage amplifier with a differential input and, usually, a single-ended output. Operational amplifier used in this case is LM741. These are general purpose OP-Amp which feature improved performance. These are simple plug in OP-Amp, hence easily replaceable. The typical OP-Amp configuration is shown below

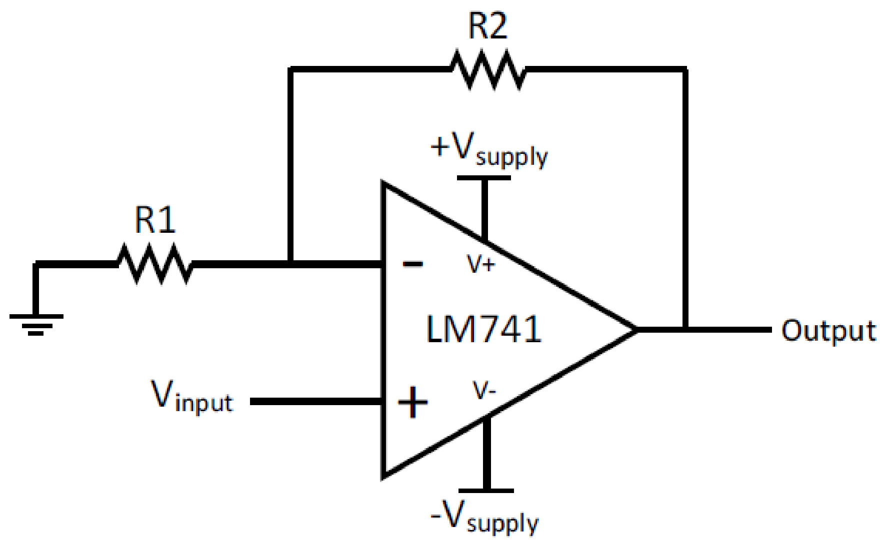

Figure 48: Typical Application

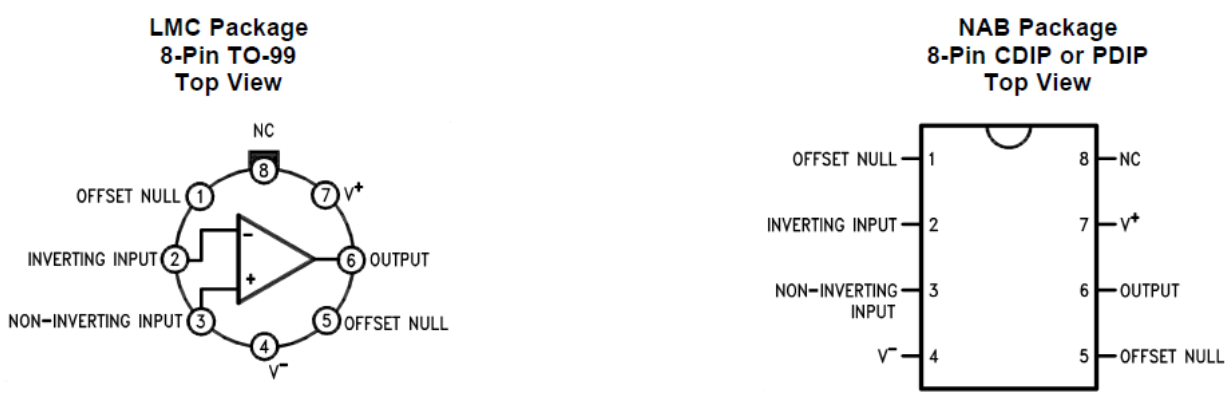

Figure 49: pin configuration and function

		MIN	MAX	UNIT
Supply voltage	LM741, LM741A		±22	V
	LM741C		±18	
Power dissipation [4]			500	mW
Differential input voltage			±30	V
Input voltage [5]			±15	V
Output short circuit duration		Continuous		
Operating temperature	LM741, LM741A	–50	125	°C
	LM741C	0	70	
Junction temperature	LM741, LM741A		150	°C
	LM741C		100	
Soldering information	PDIP package (10 seconds)		260	°C
	CDIP or TO-99 package (10 seconds)		300	°C
Storage temperature, T_{stg}		–65	150	°C

Figure 52: LM 741 Maximum Ratings

		MIN	NOM	MAX	UNIT
Supply voltage (VDD-GND)	LM741, LM741A	±10	±15	±22	V
	LM741C	±10	±15	±18	
Temperature	LM741, LM741A	–55		125	°C
	LM741C	0		70	

Figure 51: LM741 Operating Conditions

PARAMETER		TEST CONDITIONS		MIN	TYP	MAX	UNIT
Input offset voltage		$R_S \leq 10$ kΩ	$T_A = 25°C$		2	6	mV
			$T_{AMIN} \leq T_A \leq T_{AMAX}$			7.5	mV
Input offset voltage adjustment range		$T_A = 25°C$, $V_S = ±20$ V			±15		mV
Input offset current		$T_A = 25°C$			20	200	nA
		$T_{AMIN} \leq T_A \leq T_{AMAX}$				300	
Input bias current		$T_A = 25°C$			80	500	nA
		$T_{AMIN} \leq T_A \leq T_{AMAX}$				0.8	μA
Input resistance		$T_A = 25°C$, $V_S = ±20$ V		0.3	2		MΩ
Input voltage range		$T_A = 25°C$		±12	±13		V
Large signal voltage gain		$V_S = ±15$ V, $V_O = ±10$ V, $R_L \geq 2$ kΩ	$T_A = 25°C$	20	200		V/mV
			$T_{AMIN} \leq T_A \leq T_{AMAX}$	15			
Output voltage swing		$V_S = ±15$ V	$R_L \geq 10$ kΩ	±12	±14		V
			$R_L \geq 2$ kΩ	±10	±13		
Output short circuit current		$T_A = 25°C$			25		mA
Common-mode rejection ratio		$R_S \leq 10$ kΩ, $V_{CM} = ±12$ V, $T_{AMIN} \leq T_A \leq T_{AMAX}$		70	90		dB
Supply voltage rejection ratio		$V_S = ±20$ V to $V_S = ±5$ V, $R_S \leq 10$ Ω, $T_{AMIN} \leq T_A \leq T_{AMAX}$		77	96		dB
Transient response	Rise time	$T_A = 25°C$, Unity Gain			0.3		μs
	Overshoot				5%		
Slew rate		$T_A = 25°C$, Unity Gain			0.5		V/μs
Supply current		$T_A = 25°C$			1.7	2.8	mA
Power consumption		$V_S = ±15$ V, $T_A = 25°C$			50	85	mW

Figure 50: LM741 electrical conditions

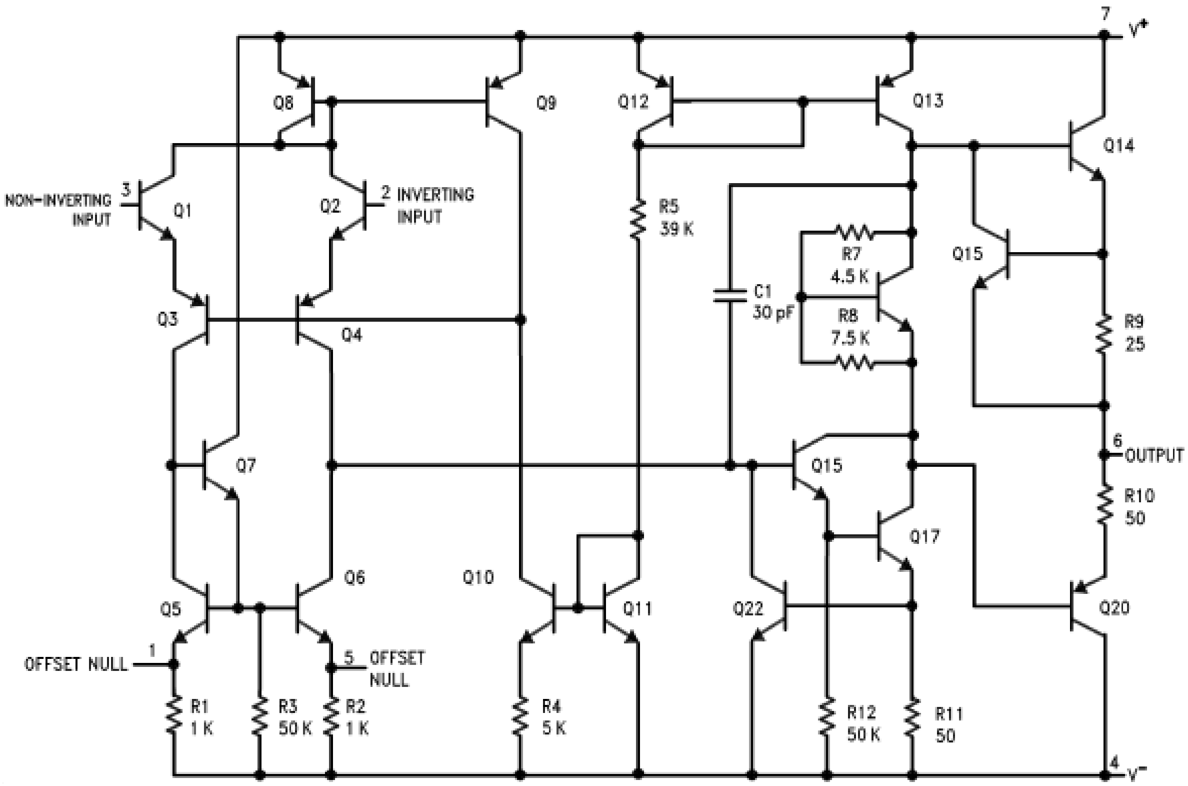

Figure 54: LM741 functional Block diagram

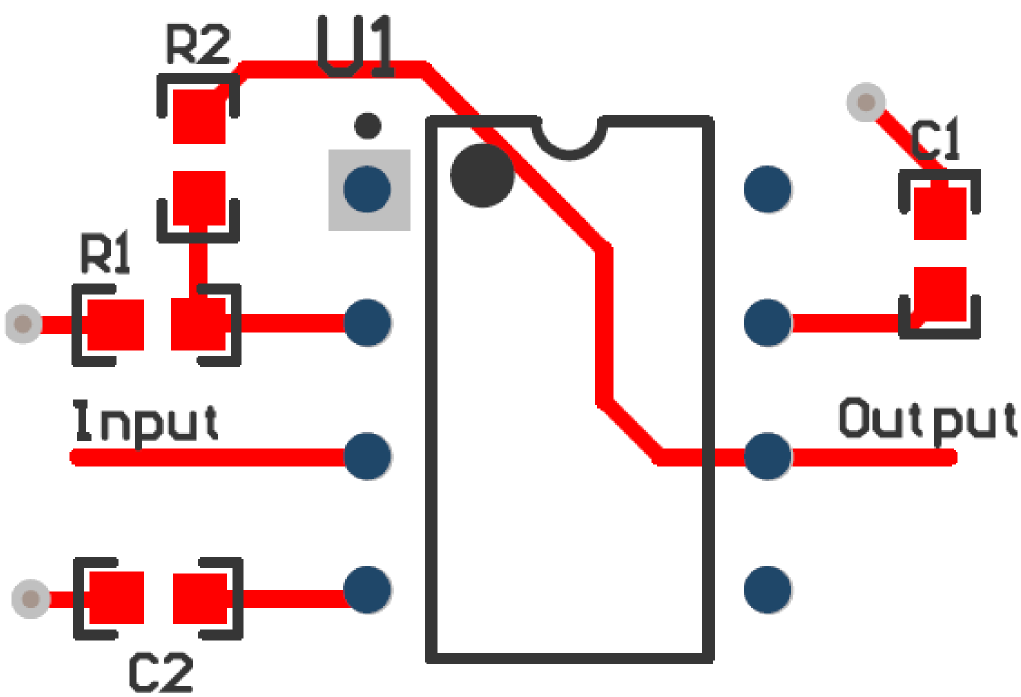

Figure 53: LM 741 layout

5.4.2 Circuit Diagram and Sensor assembly

Circuit diagram of our system connecting sensor with Operational amplifier is shown below

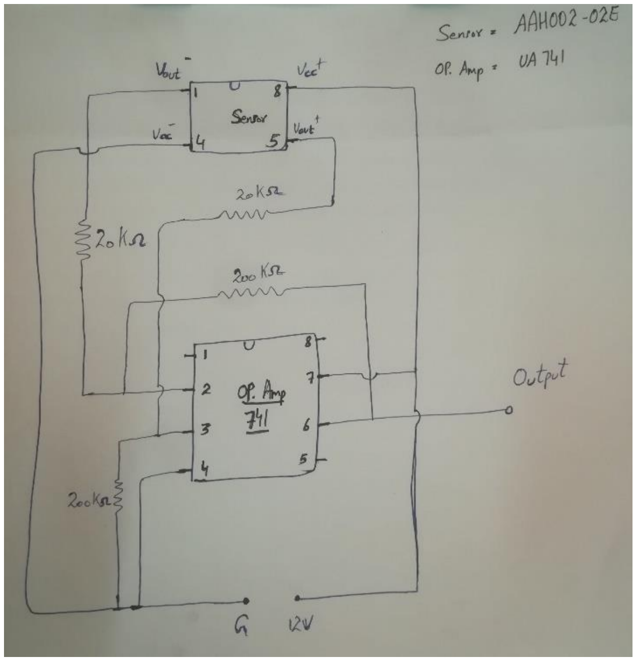

Figure 55: Hand drawn Circuit diagram

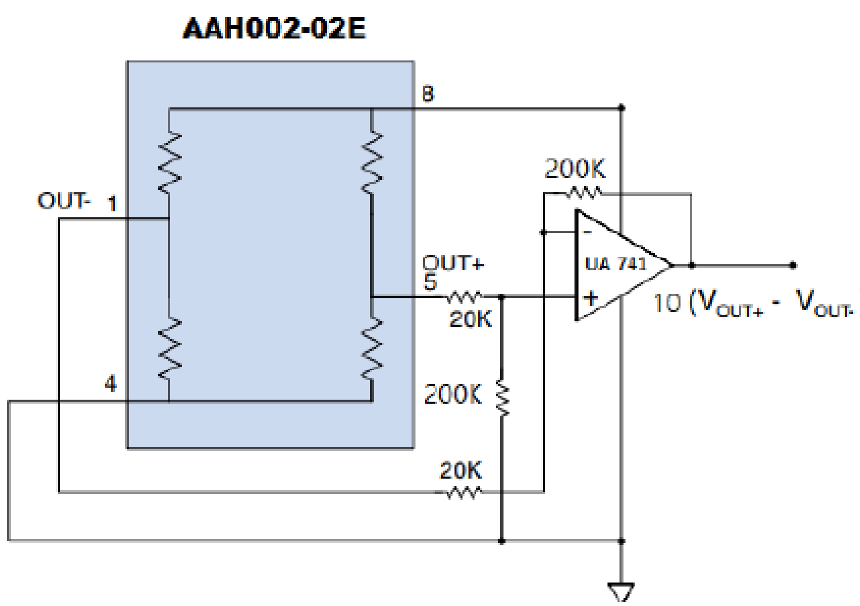

Figure 56: Circuit Diagram of the system

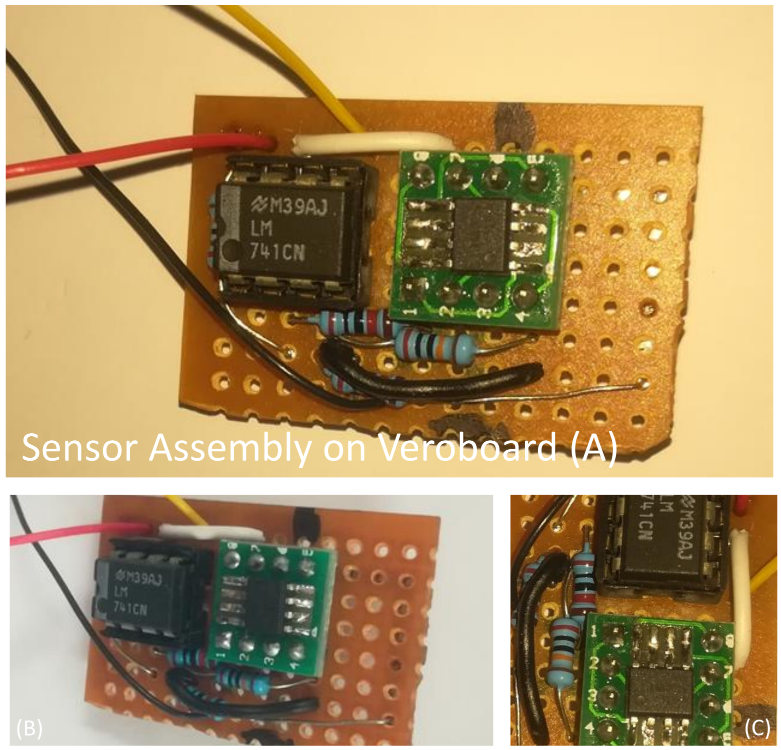

Figure 57: Sensor Assembly on Veroboard

GMR sensor in connected to operational amplifier by means of some resistors to get a gain of x10. The overall logic of the system is as follows

Figure 58: Working principle

The system is powered by a 12V power supply connected to GMR sensor which is in turn connected to operational amplifier to amplify the signal and to filter some of the noise signal and the output of the operational amplifier is connected to the data acquisition system. NI DAQ USB-6009 is used for this purpose. The details of the data acquisition system are mentioned in next section.

5.4.3 NI USB-6009

NI data acquisition card USB-6009 is used to collect the output signal into our PC. It is a multifunctional input/output (I/O) device which has both analog and digital type I/O options. Our sensor is an analog sensor so we used the analog type input option of this card. The pin configuration of the USB-6009 is shown below.

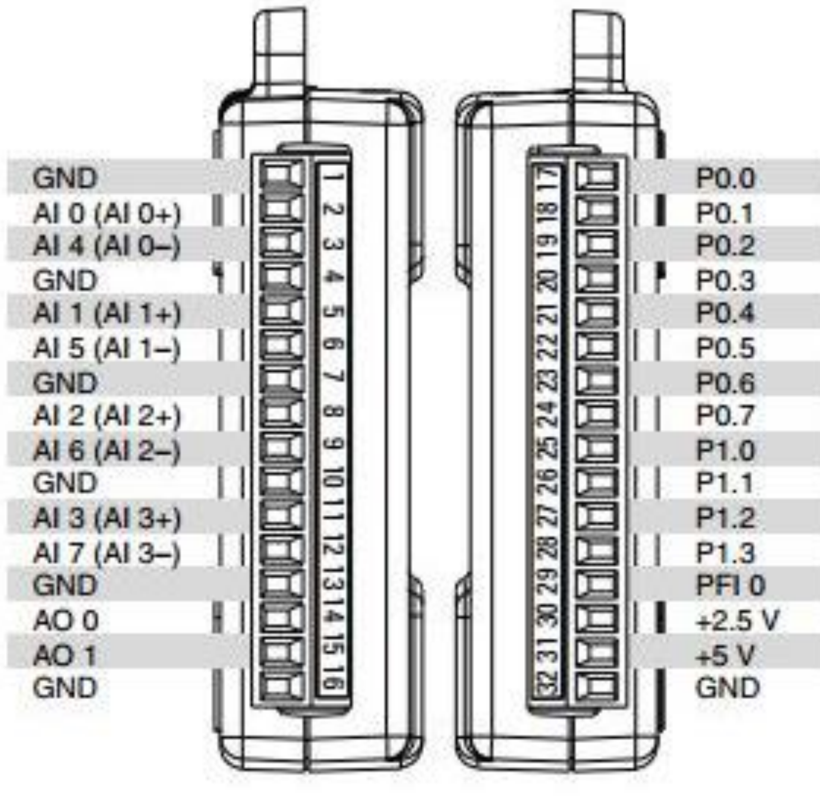

Figure 59: NI USB-6009 Pin Configuration

A LabVIEW code is generated to take the output from the USB DAQ card. The code is mentioned in the next section.

5.4.3 LabVIEW

LabVIEW program and front panel is shown below

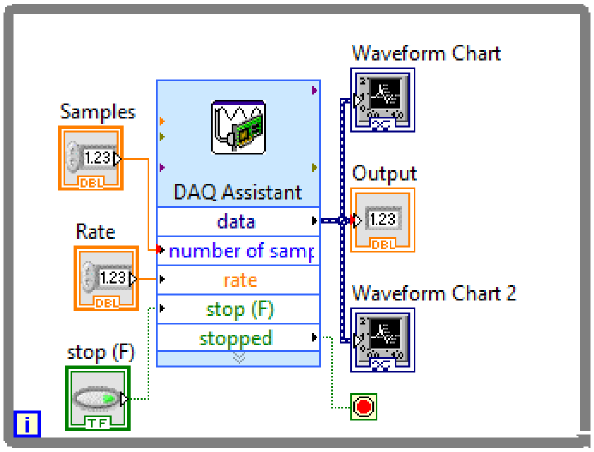

Figure 60: LabVIEW program

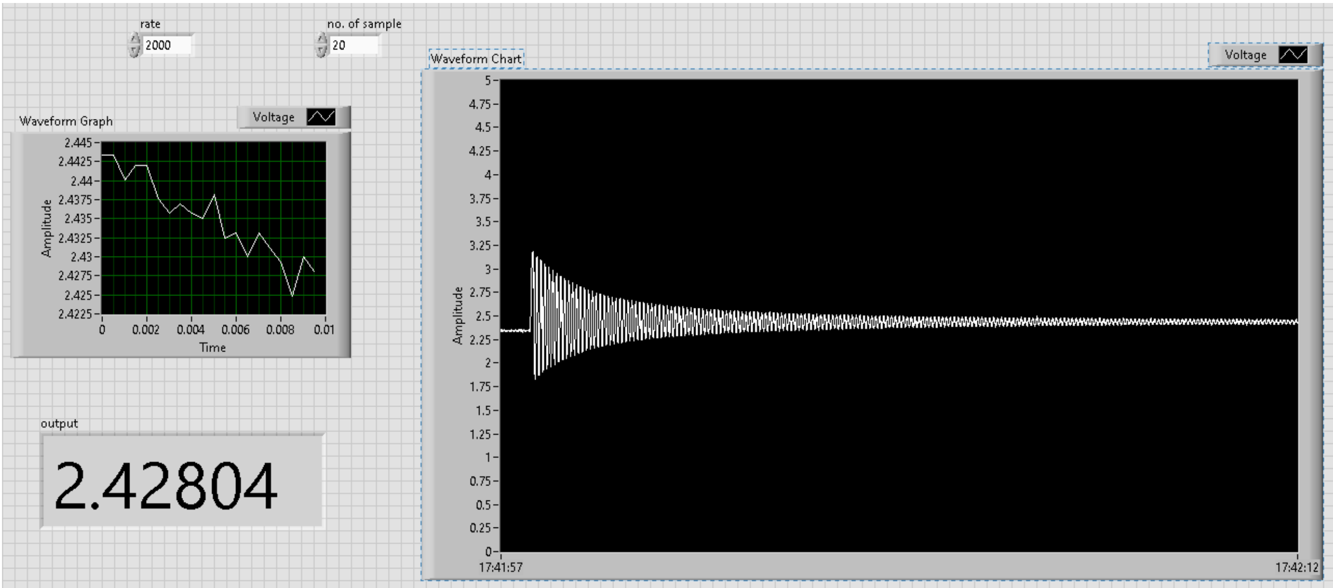

Figure 61: LabVIEW Front panel

System output is connected to LabVIEW through DAQ card. Output is presented in three different ways just for the ease of understanding.

5.5 Sensor Calibration

A PCB vise is used to calibrate the sensor as we can get precise linear motion on it. On one end of the vise, we mounted our sensor assembly while on the other side we mounted a standard magnet fig 1. Total stroke of the vise is 39.25mm meanwhile one full rotation moves it by 0.8313 mm. There are a total of 42 fins in total on ratchet of pcb vise and rotation of one fin gives us a linear movement of approximately 20microns and the average voltage change for 20 microns is 0.0047V. Using these small increments, we calibrated the sensor over entire working range which is shown in fig 3. A small ceramic magnet was used in this case. Later on, we used a standard neodymium magnet for calibration as we plan to use it in our experimentation. A complete working range for neodymium magnet was also acquired using same process

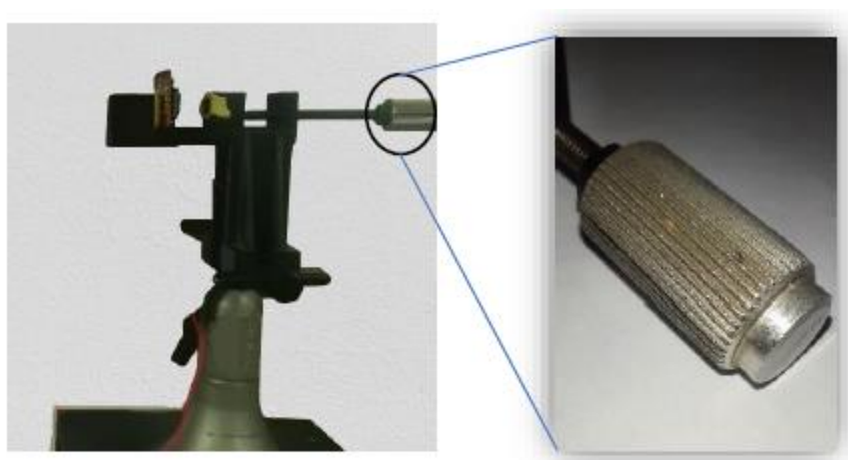

Figure 62: Calibration Setup

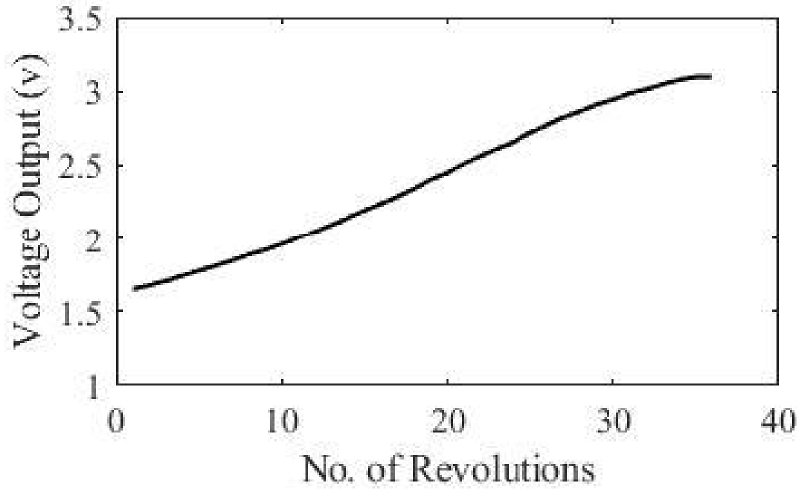

Figure 63: Graph of Voltage vs No. of revolutions of knob

Chapter 06

System Identification

6.1 System Identification toolbox MATLAB

MATLAB has a graphic user interface (GUI) for system identification in their toolbox. I used this GUI to perform system identification of my system. First you import a workable data in the toolbox and then you can process your data by applying the appropriate method out of various tools available to get to your results. I first applied the technique for a simple single degree of freedom linear system. In this system we have a simple hanging mass attached to a spring. We leave the mass from a certain height and observe the output signal from the sensor until it comes to rest. We applied the GRAYEST function in this case.

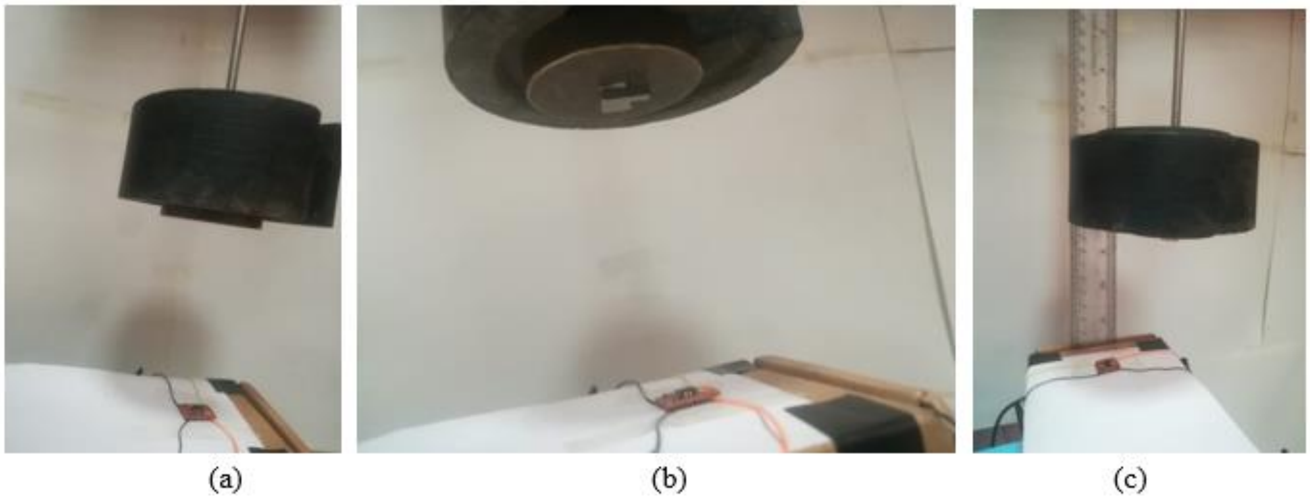

Figure 64: Single DOF hanging mass spring system

Initially, a 20N force was provided to the system as an input after which was allowed to vibrate freely. GMR sensor sensed the position of the system because of the change in magnetic field produced due to the permanent magnet attached to the hanging mass. The output of the system was as below.

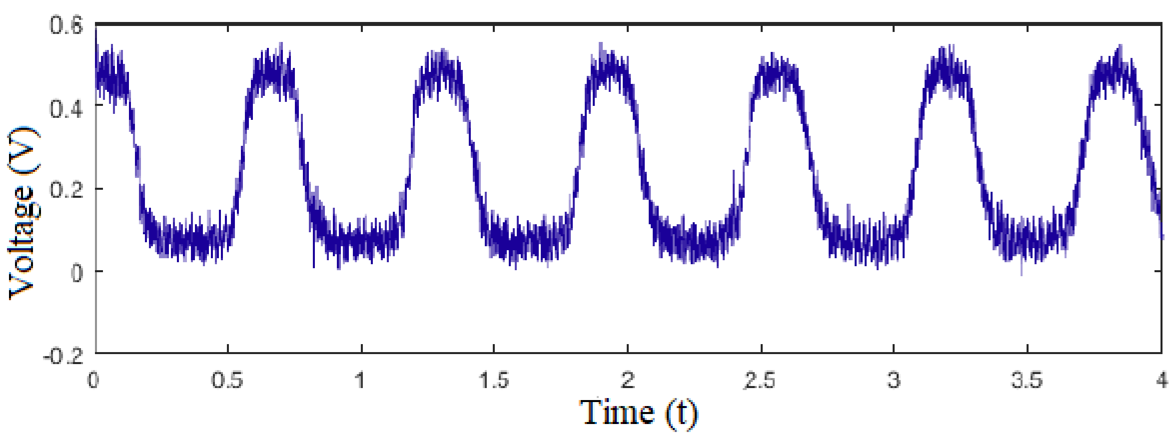

Figure 65: Output of the mass spring system

Meanwhile the input was the 20N force or step force. It is shown below

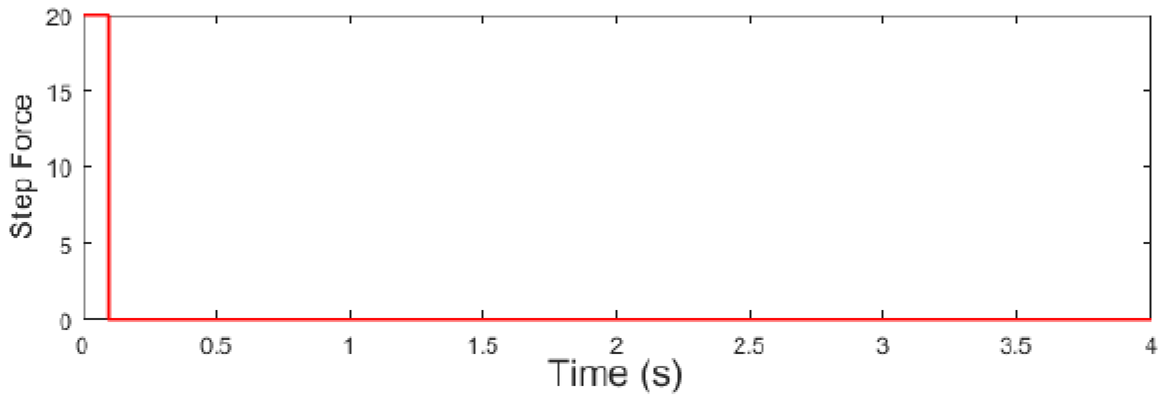

Figure 66: Input of the mass spring system

The output signal is very noisy. It is due to the non-ideal condition of the rooms where experiment is conducted. It was rectified later on by using an operational amplifier and some resistors but in this case, we simply filtered the signal to gain a simple output signal. This simplified signal looks as below.

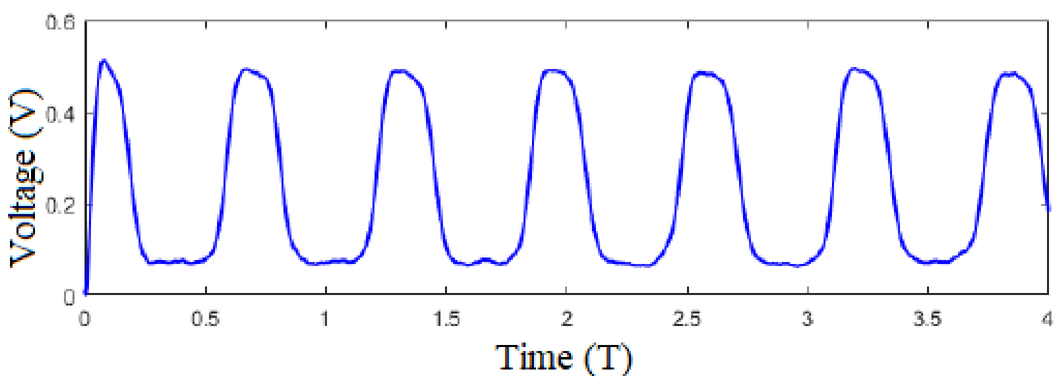

Figure 67: Filtered Output

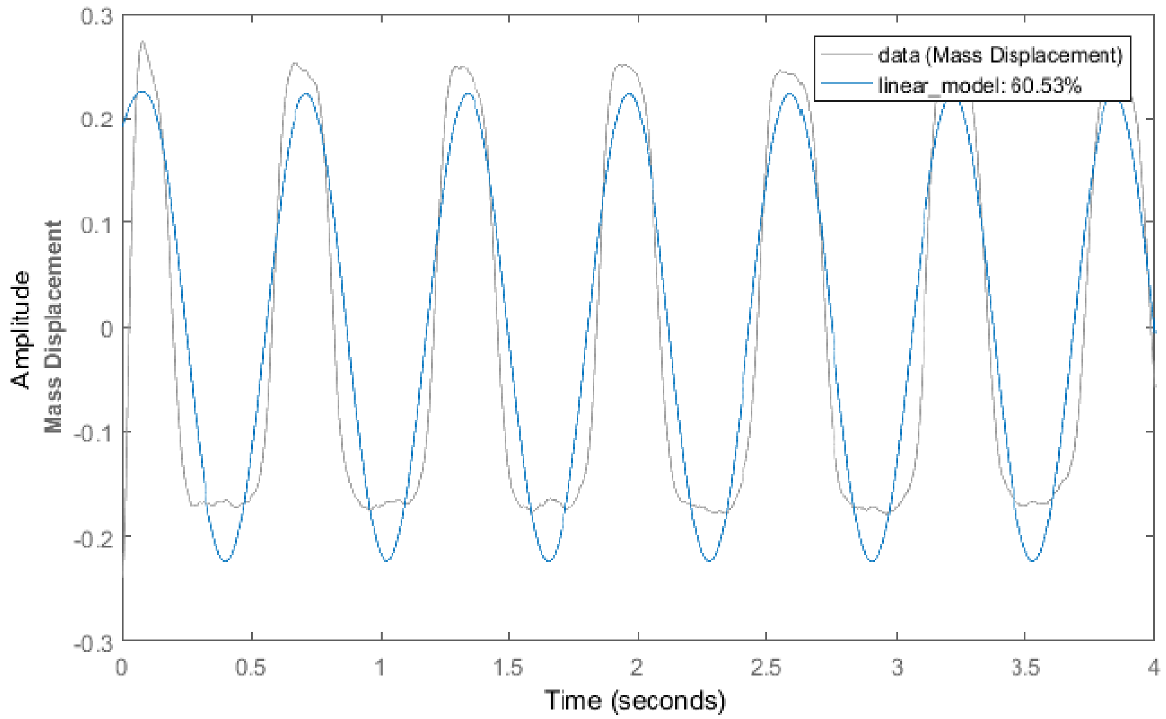

Figure 68: Comparison of system response

The system response was compared to a simulated response and a similarity of 60.53% was observed. Following were the components/data points for the system identification.

Function used	GREYEST
Input	20N Step Input
No. of Samples	4001
No. of iterations	20
Estimated parameters	Natural Frequency= 10.042 rad/s Damping = [b] = -0.001
Actual parameters	Natural Frequency= 10.1733 rad/s Damping = [b] = 0
Fit to estimation data	[60.53 %]

Figure 69: Single DOF SI problem data & results

Another data set was achieved from the following experimental arrangement and System identification tools were applied on it as well.

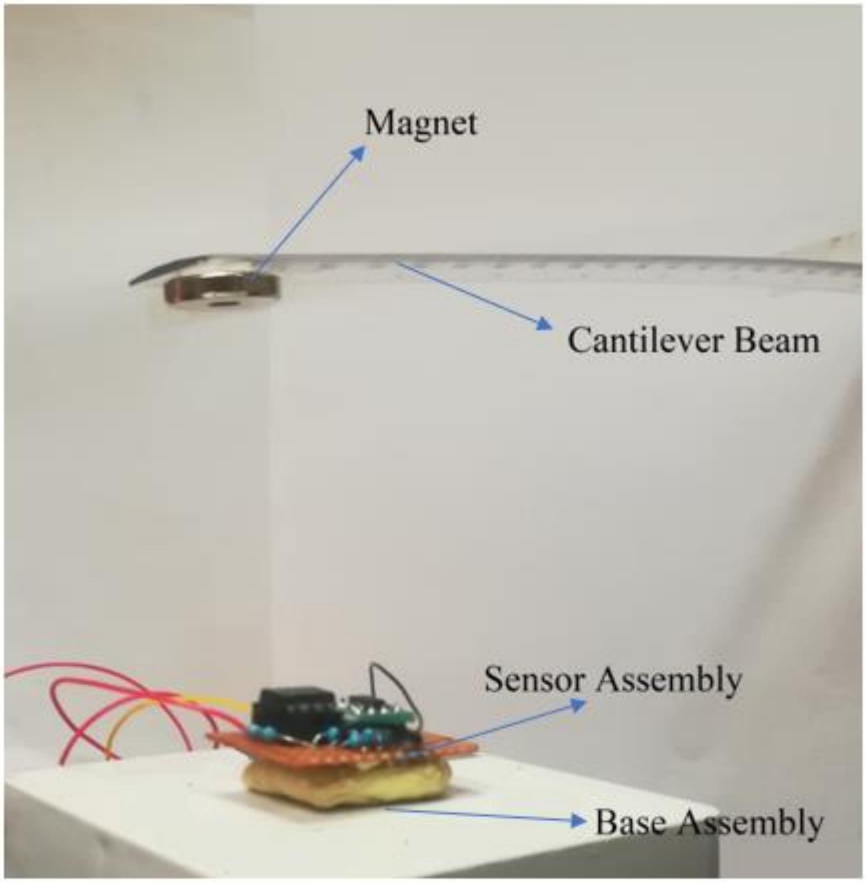

Figure 70: Sensor and magnet assembly arrangement

Chapter 07

Results & Conclusion

7.1 Method

A cantilever beam in vibration is used for this study fig 6. A magnet is mounted at the end of this cantilever beam and the sensor assembly is placed under this magnet. We calibrated the setup for one cycle but the sensor output voltage is not linear over the entire range so we divided the sensor output into linear and nonlinear parts and devised a setup this is operatable in the linear range, the graph for the sensor output is shown in fig 2. It is important to notice that voltage and distances in the graph are not absolute values but they are change in voltage and change is distance from their initial values, meanwhile initial values are considered as zero**.**

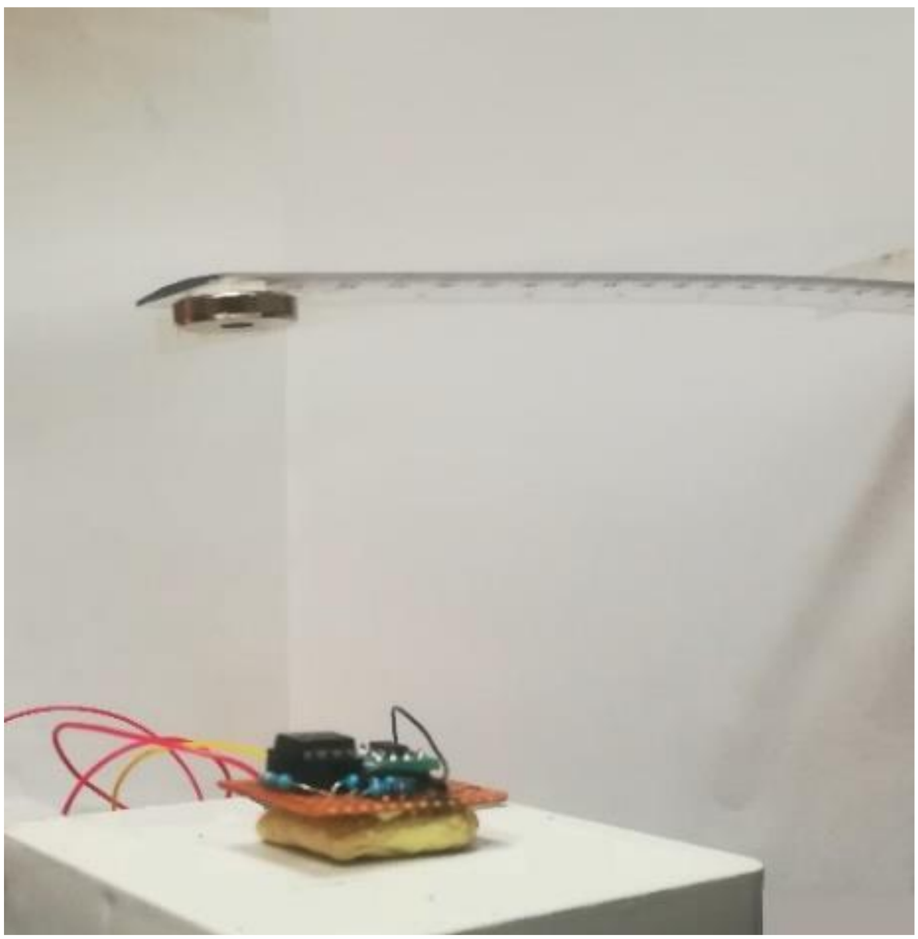

Figure 71: Experimental Setup

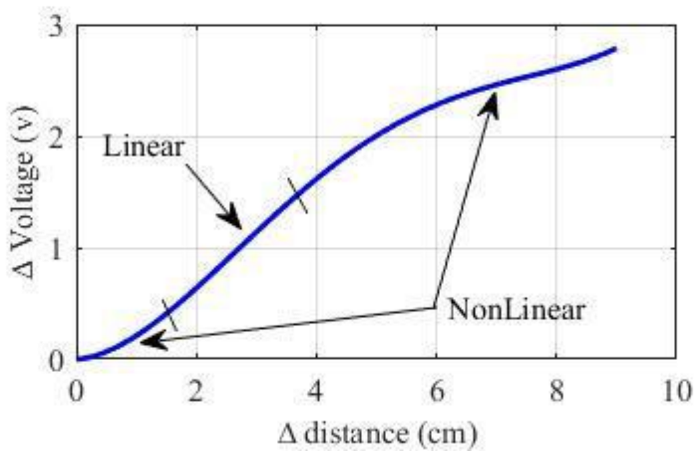

Figure 72: Voltage vs distance over entire range

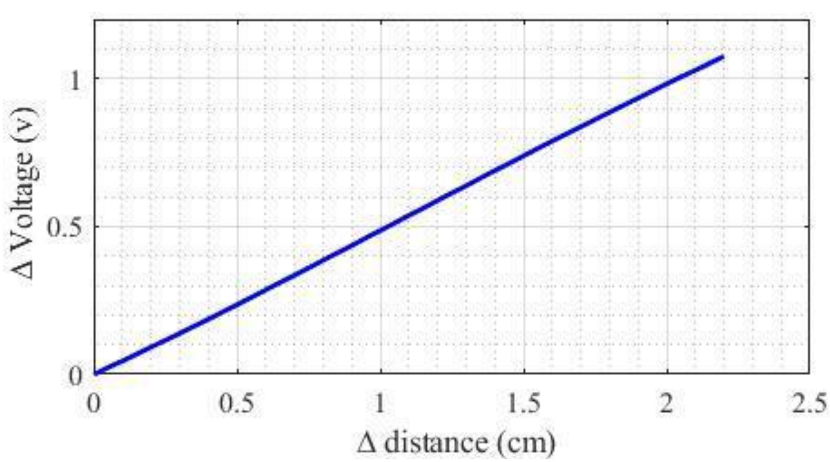

Figure 73: Voltage vs distance Linear range

GMR sensor is calibrated and a linear range is calculated for this system. Complete readings are mentioned along with validation through a stroboscope in the next section.

7.1.1Stroboscope

A stroboscope is an instrument that emits a series of brief, intense flashing lights at specific intervals. When the flashing light from a stroboscope is directed onto an object rotating at high speed, the moving fan appears to stand still.

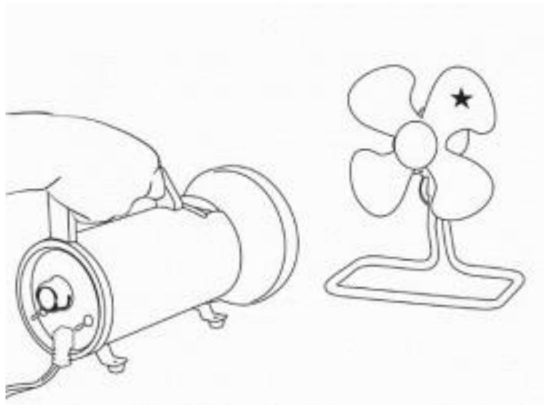

Figure 74: Stroboscope

Figure 75: Stroboscope

7.2 Results

GMR sensor AAH002-02e was calibrated over its linear range and the voltage-time output of the sensor is converted to distance-time

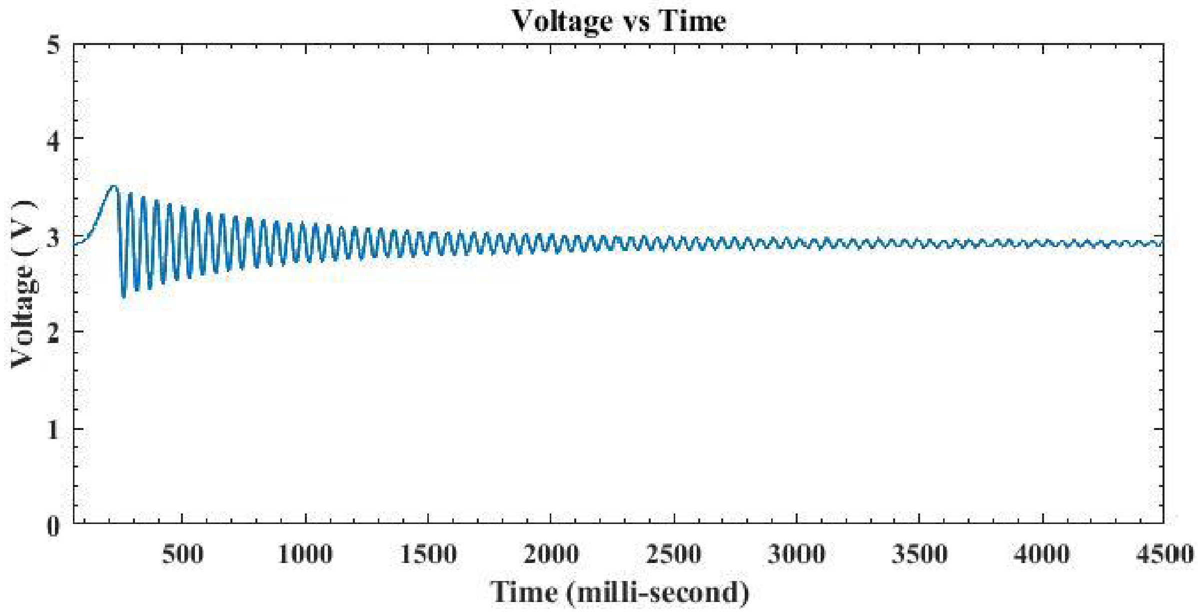

Figure 76: Sensor Output

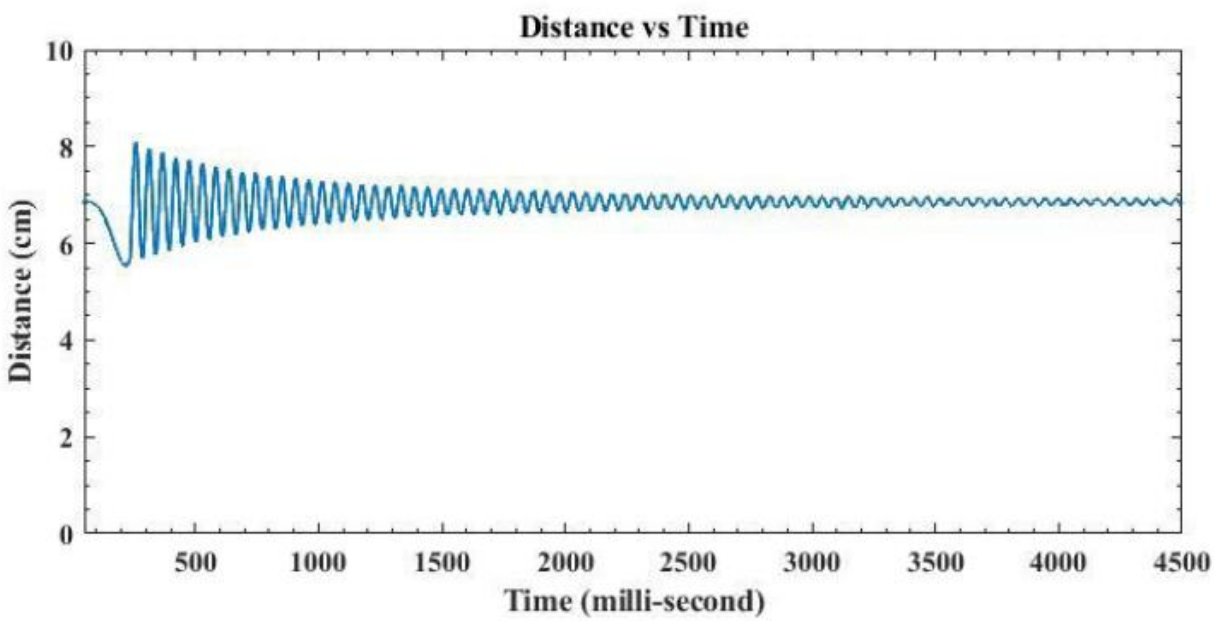

Figure 77: Voltage-Time converted to Distance-Time

7.2 Conclusion

This study focused on the GMR sensor vibration measurement for a single degree of freedom system. Different arrangements were used for the system and necessary precautions were taken as the sensor is highly sensitive to outside disturbance. An operational amplifier is introduced to magnify the system output and as a result successful measurement of a single degree of freedom cantilever beam in vibration was carried out. The voltage signal is then calibrated to get the output in terms of distance which is more perceivable. The experiment is successfully carried out and a stroboscope is used to validate the system,

References

1. Pelegri, J., Alberola, J., Lajara, R., & Santiso, J. (2007, May). Vibration detector based on GMR sensors. In Proc. IEEE IMTC (pp. 1-5).
2. Sebastiá, J. P., Lluch, J. A., Vizcaino, J. R. L., & Bellon, J. S. (2008). Vibration detector based on GMR sensors. IEEE Transactions on Instrumentation and Measurement, 58(3), 707-712.
3. NVE Corporation. AA/AB-Series Analog Magnetic Sensors. SB-00-059_RevG, July 2019. https://www.nve.com/analogSensors.
4. Mickael, P. W. (2018). A near field, non-contact vibration detector using giant magnetoresistance sensors (Doctoral dissertation, Georgia Institute of Technology). Research on vibration sensor based on giant magnetoresistance effect (2019).
5. Shejwal N. N., Gaikwad S. L., Singh P. K., Vanalakar S. A. (2022). Advances in Material Science Volume II, 36-44.
6. Daughton, J. M. (1999). GMR applications. Journal of Magnetism and Magnetic Materials, 192(2), 334-342.
7. Giebeler, C., Adelerhof, D. J., Kuiper, A. E. T., Van Zon, J. B. A., Oelgeschläger, D., & Schulz, G. (2001). Robust GMR sensors for angle detection and rotation speed sensing. Sensors and Actuators A: Physical, 91(1-2), 16-20.
8. Goh, K. M., Chan, H. L., Ong, S. H., Moh, W. P., Töws, D., & Ling, K. V. (2010, June). Wireless GMR sensor node for vibration monitoring. In 2010 5th IEEE Conference on Industrial Electronics and Applications (pp. 23-28). IEEE.
9. Gao, H., Lin, J., Zhao, Z., Zeng, R., Wang, X., Xin, Y., ... & Zhou, X. (2019). Research on vibration sensor based on giant magnetoresistance effect. Review of Scientific Instruments, 90(10), 105001.
10. Sathappan, N., Tokhi, M., Duan, F., Zhao, Z., Kaur, A., & Shirkoohi, M. (2020, December). Properties of GMR based sensor for Magnetic field measurement at increasing Temperature Conditions. In NDE 2020 India-Virtual Conference & Exhibition on Non-Destructive Evaluation.
11. Bernieri, A., Ferrigno, L., Laracca, M., & Tamburrino, A. (2007, May). Improving GMR magnetometer sensor uncertainty by implementing an automatic procedure for calibration and adjustment. In 2007 IEEE Instrumentation & Measurement Technology Conference IMTC 2007 (pp. 1-6). IEEE.
12. Bernieri, A., Betta, G., Ferrigno, L., & Laracca, M. (2013). Improving performance of GMR sensors. IEEE Sensors Journal, 13(11), 4513-4521.
13. Schott, C., Racz, R., Betschart, F., & Popovic, R. S. (2002). Novel magnetic displacement sensors. Paper No. SENSORS-00355-2002.
14. Zhang, M., Goettert, J., Lian, K., Hormes, F. J., & Ajmeraa, P. K. Superparamagnetic Particle Embedded Microprobe (SPEM) for GMR Sensor Calibration.
15. Rieger, G., Ludwig, K., Hauch, J., & Clemens, W. (2001). GMR sensors for contactless position detection. Sensors and Actuators A: Physical, 91(1-2), 7-11.
16. Pelkner, M., Neubauer, A., Reimund, V., Kreutzbruck, M., & Schütze, A. (2012). Routes for GMR-sensor design in non-destructive testing. Sensors, 12(9), 12169-12183.

17. Cubells-Beltrán, M. D., Reig, C., Madrenas, J., De Marcellis, A., Santos, J., Cardoso, S., & Freitas, P. P. (2016). Integration of GMR sensors with different technologies. Sensors, 16(6), 939.
18. Reig, C., Cardoso, S., & Mukhopadhyay, S. C. (2013). Giant magnetoresistance (GMR) sensors. Smart Sensors, Measurement and Instrumentation, 6(1), 1-301.
19. Li, Z., & Dixon, S. (2016). A closed-loop operation to improve GMR sensor accuracy. IEEE Sensors Journal, 16(15), 6003-6007.
20. Wang, L., Hu, Z., Zhu, Y., Xian, D., Cai, J., Guan, M., ... & Liu, M. (2020). Electric field-tunable giant magnetoresistance (GMR) sensor with enhanced linear range. ACS applied materials & interfaces, 12(7), 8855-8861.
21. Whitney, S. (1999). Vibrations of cantilever beams: Deflection, frequency, and research uses. Website: Apr, 23(10), 2-5.
22. To, C. W. S. (1982). Vibration of a cantilever beam with a base excitation and tip mass. Journal of Sound and Vibration, 83(4), 445-460.
23. Nardini, D., & Brebbia, C. A. (1983). A new approach to free vibration analysis using boundary elements. Applied mathematical modelling, 7(3), 157-162.
24. Lisa, K., Travis, J., Rolfson, C., & Weber, D. (1997). LabVIEW for everyone: graphical programming made even easier.
25. Bishop, R. H. (1999). Learning with labview.
26. Kalkman, C. J. (1995). LabVIEW: A software system for data acquisition, data analysis, and instrument control. Journal of clinical monitoring, 11(1), 51-58.
27. Krauß, A., Weimar, U., & Göpel, W. (1999). LabView™ for sensor data acquisition. TrAC Trends in Analytical Chemistry, 18(5), 312-318.
28. Kahneman, D., & Wolman, R. E. (1970). Stroboscope motion: Effects of duration and interval1. Perception & Psychophysics, 8(3), 161-164.
29. Frungel, F., Hiller, W. J., Meier, G. E. A., & Stasicki, B. (1985, February). High Frequency Stroboscope Using LEDs As Light Source. In 16th Intl Congress on High Speed Photography and Photonics (Vol. 491, pp. 396-399). SPIE.

System Identification of Vibrational System using GMR Sensor

ORIGINALITY REPORT

9%	9%	0%	%
SIMILARITY INDEX	INTERNET SOURCES	PUBLICATIONS	STUDENT PAPERS

PRIMARY SOURCES

1	hdl.handle.net Internet Source	5%
2	en.wikipedia.org Internet Source	3%

Exclude quotes	On	Exclude matches	< 3%
Exclude bibliography	On		